MATERIALS CHEMISTRY
FRONTIERS

REVIEW

View Article Online
View Journal | View Issue

Cite this: *Mater. Chem. Front.*, 2023, **7**, 355

Synergistic photothermal antibacterial therapy enabled by multifunctional nanomaterials: progress and perspectives

Xiaotian Bai,[a] Yue Yang,[a] Wen Zheng,[b] Yue Huang,[a] Fanxing Xu*[b] and Zhihong Bao *[a]

In recent years, infection caused by drug-resistant bacteria has become a serious public health problem. The exploration of antibacterial therapies other than antibiotics has attracted more and more attention. Photothermal therapy (PTT) has become a promising antibacterial method due to its low invasiveness, low toxicity and avoidance of drug-resistant bacteria. However, when PTT is used alone, it requires a higher temperature to achieve a better antibacterial effect, which will not only kill bacteria, but also cause damage to normal tissues, and even trigger new inflammation. Many reports have confirmed that a combination of other antibacterial methods with PTT could effectively reduce the side effects on normal cells and enhance the therapeutic effect. In view of the rapid development of synergistic PTT in antibacterial therapy, this review mainly discusses and summarizes the advancements of several synergistic photothermal antibacterial methods within the last five years. In addition, the synergistic mechanism of antibacterial methods is also clarified. The remaining challenges and future opportunities in this field are also highlighted. We believe that this review will provide improved understanding of synergistic photothermal antibacterial therapy enabled by multifunctional nanomaterials and push nanoscience and nanotechnology one step at a time toward clinical applications.

Received 6th November 2022,
Accepted 14th December 2022

DOI: 10.1039/d2qm01141g

rsc.li/frontiers-materials

1. Introduction

Bacterial infection has been a globally deterring threat to human well-being by causing many diseases such as pneumonia, meningitis, sepsis, cholera, skin ulcer, and gastric cancer.[1] For example, *Staphylococcus aureus* (*S. aureus*) and *colon bacillus* are widely present in nature and can easily cause pneumonia, food poisoning and other diseases in people.[2] In addition, after

[a] *School of Pharmacy, Shenyang Key Laboratory of Functional Drug Carrier Materials, Shenyang Pharmaceutical University, Shenyang, 110016, P. R. China. E-mail: zhbao@syphu.edu.cn*
[b] *Wuya College of Innovation, Shenyang Pharmaceutical University, Shenyang, 110016, P. R. China. E-mail: fanxing0011@163.com*

Xiaotian Bai

Xiaotian Bai received her BS degree in Pharmaceutics from Shenyang Pharmaceutical University in 2021. She is currently pursuing her MS in Pharmaceutics at Shenyang Pharmaceutical University. Her current research focuses on the preparation of biodegradable nanoparticles for chemo-photothermal antibacterial and anti-tumor therapy.

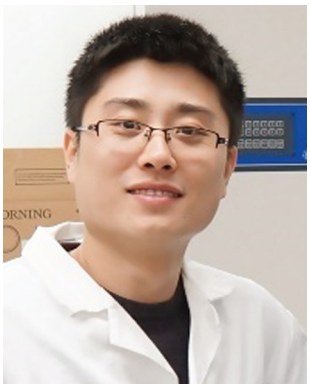

Fanxing Xu

Prof. Fanxing Xu received his PhD degree in biochemical engineering from Dalian University of Technology in 2014. Then he joined Shenyang Pharmaceutical University as a lecturer and was promoted as an associate professor in 2018. His current research interests focus on the pathophysiology and treatment of diabetes and its complications.

surgical treatment the implantation of bacteria on the surface of wounds seriously threatens human health and is a major obstacle in the treatment of diseases.[3] To address these severe issues, antibiotics,[4,5] antimicrobial peptides,[6,7] and quaternary ammonium compounds[8,9] have been researched and widely used. Among them, antibiotics as effective antimicrobial drugs are extensively developed. However, the frequent use of antibiotics will make bacteria drug resistant. The emergence of an increasing number of drug-resistant bacteria leads to an increase in the mortality rate of many diseases, which is called the abuse of antibiotics. The main mechanisms of antibiotic resistance are as follows:[10,11] (1) long-term use of antibiotics or the presence of polymers within the biofilm reduces the permeability of the bacterial cell membrane, limiting the entry of antibiotics; (2) the overexpression of the bacterial efflux pump, allowing antibiotics to be ingested and then excreted; (3) enzymes within the bacteria degrade antibiotics; (4) the change in the metabolic pathways of the bacteria inhibit the antibacterial efficiency of the antibiotic; and (5) attacks by the host's immune system. At present, drug-resistant bacterial infections cause 700 000 deaths every year.

If urgent attention is not paid, the total number of deaths will rise to 10 million per year in 2050.[12] The discovery of new antibiotics is far slower than the increase in drug-resistant bacteria, which is now recognized as a serious problem in the medical field and in our living environment. Therefore, it is expected to explore a new, safe and effective non-antibiotic treatment strategy, that does not produce drug-resistant bacteria and avoids damage to normal cells while killing bacteria in the body.[13]

In recent years, photothermal therapy (PTT) has been considered as a promising way for anti-bacterial, disinfection, and tumor treatment due to its peculiar merits such as non-invasiveness, targeted selective treatment, and minimized side effects.[14,15] Photothermal antibacterial therapy (PTAT) is a method to induce bacterial damage by generating heat in the presence of therapeutic agents and suitable light sources.[16]

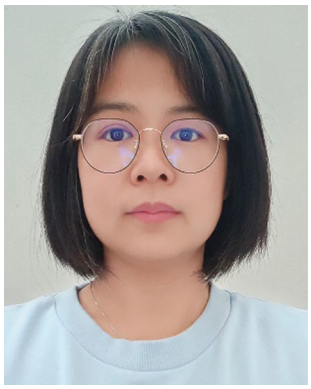

Zhihong Bao

Prof. Zhihong Bao received her PhD degrees in physical chemistry from Jilin University in 2003 and 2008. Then she was a Postdoctoral Research Fellow in the Chinese University of Hong Kong from 2009 to 2010. She is currently an associate professor at the School of Pharmacy, Shenyang Pharmaceutical University. Her current research interests mainly focused on the controllable synthesis and application of multifunctional nanomaterials for photothermal antitumor and antibacterial therapy.

PTAT refers to a physical antibacterial method. In PTAT, antibacterial agents can increase their own temperature under near-infrared (NIR) light irradiation, and the increase in temperature can effectively kill bacteria through a variety of thermal effects such as cell membrane rupture, protein/enzyme degeneration, cell hollowing, and cell fluid evaporation.[17] PTAT has a broad spectrum of antibacterial effects, and will not induce bacteria to develop drug resistance. Moreover, NIR light between 700 and 1400 nm has good tissue penetration ability, and can penetrate the skin without causing damage, and even reach deep tissues for thorough antibacterial treatment. At present, photothermal antibacterial nanomaterials mainly include carbon-based nanocomposites,[18,19] metal and metal semiconductor materials,[20,21] and organic polymers.[22,23] Considering that the occurrence and development of bacteria are complex biological processes involving multiple factors and steps, the therapeutic effect of single PTT is still far from satisfactory. To achieve effective antibacterial efficacy, single PTT usually requires a temperature of more than 60 °C or higher to kill bacteria. However, high temperature or long-term exposure to hyperthermia may cause thermal damage to normal tissues around bacteria, and even trigger new inflammation.[24] Therefore, it is urgent to develop safer and more efficient PTAT strategies for rapid antibacterial therapy, *i.e.* PTAT with a lower temperature (around 50 °C) or a shorter treatment time. Recent investigations have elaborated that combining PTAT with other treatments is a promising direction to play a synergistic role in improving antibacterial activity, which can improve the antibacterial efficiency, shorten the antibacterial time, and reduce the side effects of different methods on the human body when used alone. Nanomaterials have lighter, higher and stronger properties. Lighter means that nanomaterials with small particle sizes but unchanged performance can be prepared to reduce the volume of materials and obtain a lighter nanoplatform. Higher means that nanomaterials have a smaller particle size, a larger surface area, and higher response to light, acoustics, electricity, magnetic, *etc.* At the same time, nanomaterials with small particle sizes have higher penetration into tissues and can reach deeper tissues, giving full play to the therapeutic effect. Stronger means that nanomaterials have stronger mechanical properties. Some flaky nanomaterials can destroy the cell membranes of bacteria through sharp edges and thus play an antibacterial role.

Synergistic PTAT mainly includes photodynamic–photothermal therapy, chemo-photothermal therapy, and nitric oxide (NO)–photothermal therapy. Photodynamic–photothermal antibacterial therapy refers to the combination of PTT and photodynamic therapy (PDT) that can kill bacteria with high temperature and reactive oxygen. Chemo-photothermal antibacterial therapy refers to the treatment of PTT combined with chemicals such as metal ions and antibiotics. NO–photothermal antibacterial therapy refers to the combination of photothermal agents (PTAs) with NO donor materials to realize higher bactericidal efficiency. In recent years, some excellent reviews have summarized the state-of-the-art PTAT for antibacterial therapy,[25–27] but there are few specialized reviews about synergistic PTAT for antibacterial therapy. Therefore, in this review, we summarize recent advances in synergistic PTAT

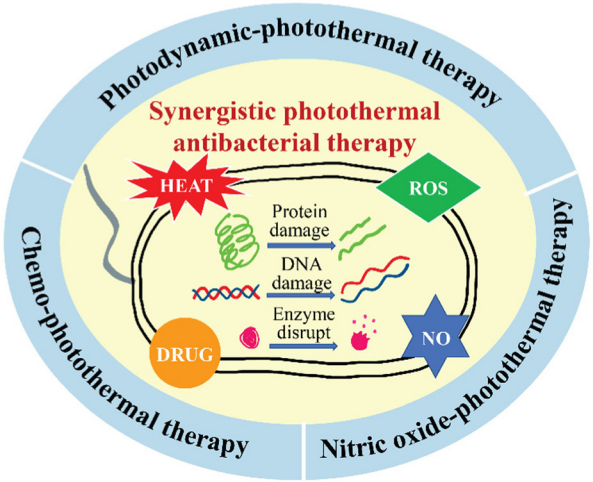

Fig. 1 Illustrative overview and the existing antibacterial mechanisms of the three synergistic photothermal antibacterial therapies.

in the last five years, including photodynamic–photothermal therapy, chemo-photothermal therapy, and NO–photothermal therapy (Fig. 1). In addition, synergistic therapeutic strategies by combining PTT with novel techniques, such as sonodynamic therapy (SDT) and immunotherapy, are briefly introduced. The synergistic mechanism of the two treatment methods is thoroughly clarified. Finally, the challenges in using synergistic PTAT in practical antibacterial applications and future perspectives are discussed. We hope that this review will help to further develop safer and more efficient antibacterial technology and push nanoscience and nanotechnology one step at a time toward clinical applications.

2. Several synergistic photothermal antibacterial methods

In recent years, NIR laser-induced PTT has attracted much research attention in biotechnology. PTAT is an important antibacterial approach that refers to the efficient generation of heat by PTAs under NIR light irradiation at an appropriate power density to kill bacteria. NIR-responsive PTAs are preferred for antibacterial therapy due to their deep biological tissue penetration capability and minimal damage to healthy tissues. During the PTAT process, bacterial cell walls become wrinkled and damaged due to the high local temperature followed by the disruption of the cell membrane. Finally, the leakage of intracellular material leads to cell death.[28,29] However, single PTAT takes a long time to kill bacteria by increasing temperature alone, and even causes damage to normal tissues around bacteria due to the influence of long-term high temperature, resulting in a series of side effects and affecting the therapeutic effect. However, a large number of studies showed that when using PTAT in combination with other antibacterial therapies, the advantages of the two treatment methods can complement each other and learn from each other's strengths, which may achieve the effect of "1 + 1 > 2". In this section, versatile properly designed practices of PTT combined with other therapies are comprehensively summarized and their superior *in vitro* and *in vivo* germicidal performances are discussed, as presented in Table 1.

2.1 Synergistic photodynamic–photothermal antibacterial therapy

Photodynamic therapy (PDT) is a treatment for nanomaterials to produce reactive oxygen species (ROS) such as hydroxyl radicals ($^{\bullet}OH$), singlet oxygen ($^1O_2$) or superoxide radicals ($^{\bullet}O^{2-}$) under laser irradiation.[30,31] Photodynamic antibacterial therapy (PDAT) refers to a process where photosensitive agents are stimulated by light to produce a large number of electrons, which are captured by the surrounding oxygen atoms or water to produce free radical oxygen species, thus quickly kill bacteria by oxidizing the proteins in bacteria and destroying bacterial membranes.[32] Ultra-strong oxidation reactions are carried out on bacteria for the treatment of diseases. However, a single PDAT, like a single PTAT, will require large amounts of ROS to kill bacteria. On the other hand, excess ROS can also cause inflammation, fibrosis, and necrosis of normal cells.[33,34] Therefore, the immense potential of a synergistic antibacterial strategy between PTAT and PDAT is considered because non-oxygen-dependent PTAT can generate heat under NIR light irradiation to make up for the efficiency inhibition caused by long time PDAT to achieve a better sterilization effect. Specifically, PTAT can reduce cell activity by raising the appropriate temperature, making cells more sensitive to the ROS generated by PDAT, and making cells more likely to inactivate.[35] In addition, the integration of multiple antibacterial mechanisms into one has the advantage of shortening the antibacterial time, improving the antibacterial efficiency, and reducing the dose of antibacterial agents. In this section, we introduce several antibacterial agents for photodynamic–photothermal antibacterial therapy.

Carbon-based materials have received increasing attention as antibacterial agents in recent years due to their good biocompatibility and environmentally benign nature.[36] Among them, graphene nanomaterials are widely used in PTAT. It is believed that the sharp edges of graphene-based nanomaterials can destroy the lipid bilayer of bacteria and achieve sterilization of abscesses.[37] Both graphene oxide (GO) and reduced graphene oxide (RGO) have broad-spectrum antibacterial activity, but Gram-negative bacteria are less sensitive to graphene nanomaterials than Gram-positive bacteria due to the protective effect of the outer membrane of Gram-negative bacteria.[38] In addition, graphene nanomaterials can also act as an electron acceptor, blocking the transfer of electrons in the electron transport chain and leading to adenosine triphosphate (ATP) exhaustion and cell death.[39] GO is a two-dimensional nanomaterial oxidized from graphene. It can act as a "nanoknife" to destroy the protein structure in the cell membrane, leading to functional failure of the protein. Moreover, GO can absorb NIR light and convert it into heat or ROS, causing irreversible cell destruction. However, due to the fast recombination rate of electrons and holes in GO, the PTT and PDT effects of GO are

Table 1 Photothermal-derived multimodal synergistic antibacterial therapy

Synergistic treatments	Examples	Outcome	Ref.
PDT–PTT	GO-Tob@CuS	Go-Tob@CuS could irreversibly destroy bacterial membranes through nanoknives, enhance PTT and PDT effects, and lead to bacterial death.	40
	Cu-RCDs-C_{35}	Cu-RCDs-C_{35} + laser group had a better effect on promoting wound healing, the photothermal antibacterial properties of CDs with high biocompatibility could be improved by doping metal ions.	42
	AuNRs@Cur	Under dual exposures of 405 nm and 808 nm, the inhibition rate of *S. aureus* and *E. coli* AuNRs@Cur was higher than that of Cur or PDT alone; the reactive oxygen and thermal energy produced by double wavelength (405 + 808 nm) laser irradiation could destroy bacterial outer membrane structure and cause bacterial death.	44
	Au@Bi_2S_3	Au@Bi_2S_3 core–shell structure had a stronger antibacterial ability compared to Au NRs or Bi_2S_3 NPs alone, which might be related to the higher ROS yield and high temperature.	46
	MoS_2/ICG/Ag	The developed MoS_2/ICG/Ag triple bactericidal system (including PTT, PDT and chemotherapy) showed a good synergistic effect in inhibiting biofilm formation and killing deep biofilm bacterial cells.	49
	PATA-C4@CuS	PATA-C4@CuS with PTT, PDT, and membrane-targeted ligands showed potential for the elimination of the bacteria.	51
	CuS nanosheet with V_s	CuS nanosheet (CuS-3) with more V_s and a narrower band gap, which was favorable for enhanced light absorption and electron transfer efficiency, had the highest PCE and ROS level.	53
	PAM–PDA/Ag@AgCl	The new phototherapy system could quickly heal bacteria-infected wounds at a relatively low temperature (52.1 °C) and moderate production of ROS.	55
	TP-Por CON@BNN6	TP-Por CON@BNN6 integrated PTT, PDT and NO therapy in one nanoplatform, the combined application of PDT + PTT + GT could increase the expression of α-SMA and CD31, suggesting that these repair cytokines effectively promoted the formation of collagen fibers and neovascularization.	58
Chemo-PTT	IMP/IR780@TRN	In TRIDENT, NIR-irradiated IR780 molecules could convert light energy into heat to mediate the lysis of MRSA by denaturing the bacterial membrane proteins/enzymes and disturbing their membrane integrity.	60
	Pd–Cu@AMO@ZIF-8	The designed NIR/pH double-stimuli-response MOF-based antibacterial agents not only successfully solved poor targeting of certain antibiotic, but also offered a promising nanoplatform for efficient antibacterial treatment.	68
	Cip-Ti_3C_2 TSG	In the MRSA-induced mouse abscess model, hybrid hydrogel had both ability of high-efficiency sterilization and long-term inhibition, avoiding bacterial rebound after photothermal treatment, thus maximizing the *in vivo* therapeutic effect of the Ti_3C_2 MXene system.	72
	Ag^+-GCS-PDA@GNRs	Ag^+-GCS-PDA@GNRs combined chemotherapy with thermotherapy could completely remove abscesses and promote wound healing through synergistic antibacterial effects.	78
NO-PTT	TG-NO-B	TG-NO-B could selectively bind to Gram-negative bacterial cells and their biofilm matrix through covalent coupling between BA groups and bacterial LPS units, thus greatly improving antibacterial efficiency and reducing adverse side effects on surrounding healthy tissues.	81
	Fe_3O_4@PDA@PAMAM@NONOates	The antibacterial activity of Fe_3O_4@PDA@PAMAM@NONOates was further enhanced by NO loading, with the aid of the excellent magnetic properties of Fe_3O_4@PDA@PAMAM@NONOates, almost all of the bacteria could be removed by the external magnet in 15 min, as the supernatant turned from the initial turbid suspensions to clear solutions.	83
	MoS_2-BNN6	The photothermal and temperature-enhanced catalytic effects of MoS_2-BNN6 + NIR conferred a synergistic PTT/NO antibacterial activity to the nanocarrier, leading to enhanced oxidative/nitrosative stress and even DNA damage; the acceleration of the oxidation of GSH, thus reducing the removal of ROS/RNS generated in bacteria, thus rapidly enhancing the biocidal effect.	84
	GNS/HPDA-BNN6	The combinational photothermal and NO treatment (GNS/HPDA-BNN6 + NIR) exerted the most significant elimination effect on the MRSA biofilm.	85
New treatment – PTT	Ag_2O_2 NPs	Ag_2O_2 NPs catalyzed H_2O_2 to produce $^{\bullet}OH$ through Fenton-like reactions and showed attractive photothermal conversion ability and good photothermal stability under NIR light, it could have effect in deeper tissues by SDT to improve antibacterial effect.	94
	Nano neuro-immune blockers (NNIBs)	NNIBs were obtained by modifying an immune escape membrane exterior on the surface of the Au nanocages, NNIBs could target the toxins produced by *S. pyogenes* so as to neutralize SLS, inhibit pain conduction, and enhance the host immune defense for invasive bacterial infection.	96
	GO/NCD/Hap	GO/NCD/Hap combined PTT with immune promotes the migration and proliferation of cells, and promotes the enhancement of alkaline phosphatase, thus facilitating tissue reconstruction.	97

seriously reduced. To overcome this problem, CuS nanoparticles were used to modify GO and to form hybrid nanoplatforms (GO@CuS), which may promote the separation efficiency of photoelectrons and holes of GO. GO (−45.2 mV) presented negative charges, so it could not penetrate the lipid bilayer of the cell membrane in a short time, reducing the antibacterial efficiency of GO@CuS. Tobramycin (Tob) is a broad-spectrum aminoglycoside antibiotic that interacts well with bacterial cell membranes through ion interactions. Thus, Tob was selected to modify GO sheets and to ensure that the carboxyl groups on GO sheets were completely consumed (Fig. 2(a)).[40] After modification, the zeta potentials of GO-Tob and GO-Tob@CuS increased

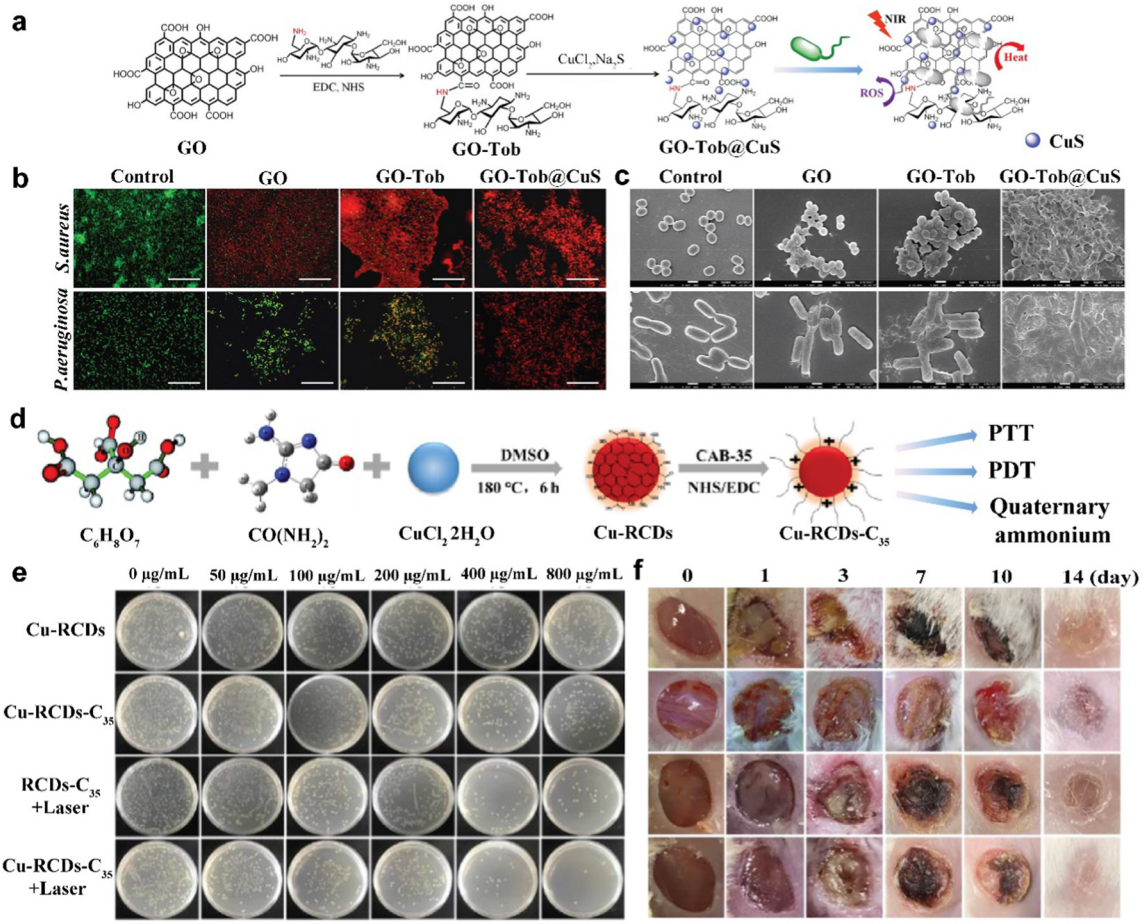

Fig. 2 (a) Schematic illustration of the synthesis of GO-Tob@CuS. (b) Fluorescence micrographs of bacteria after being treated with PBS, GO, GO-Tob and GO-Tob@CuS under NIR laser irradiation (the scale bar is 75 μm). (c) SEM images of bacteria after treatment with PBS, GO, GO-Tob and GO-Tob@CuS under NIR laser irradiation (the scale bar is 1 μm). Reprinted with permission of ref. 40. Copyright 2018 Royal Society of Chemistry. (d) Schematic illustration of the preparation of Cu-RCDs-C_{35} and related biological applications. (e) Photos of bacterial colonies of *E. coli* after being treated with Cu-RCDs, Cu-RCDs-C_{35}, RCDs-C_{35} + laser, and Cu-RCDs-C_{35} + laser. (f) Photographs of infected wound tissues from the wound areas of different treatment groups. Reprinted with permission of ref. 42. Copyright 2021 Elsevier.

to 32.3 mV and 17.3 mV, respectively. The electropositivities of GO-Tob and GO-Tob@CuS were beneficial in enhancing antibacterial efficiency through electrostatic interactions with electronegative bacterial. After 5 min under NIR lasers (980 nm, 1.5 W cm^{-2}), the temperature of the GO-Tob@CuS solution with 100 μg mL^{-1} (65 °C) was the highest, indicating that GO-Tob@CuS had excellent photothermal conversion capabilities. The production of ROS was determined using dichlorofluorescein diacetate (DCFH-DA). After NIR laser irradiation, GO-Tob@CuS presented much higher fluorescence intensity than GO-Tob, GO and CuS nanoparticles under the same conditions. This was possibly because CuS nanoparticles modified on the surface of GO can obviously improve PDT efficiency and sufficiently generate ROS under NIR laser irradiation. These results confirmed that the photodynamic and photothermal effects of GO-Tob@CuS were boosted after being modified by CuS nanoparticles. The antibiotic-resistant *Pseudomonas aeruginosa* (*P. aeruginosa*) and *S. aureus* were as models, after treated with GO-Tob@CuS for 1 h, all bacteria was found at the bottom of an optical cuvette, which was attributed to the electrostatic interaction between GO-Tob@CuS and the bacteria. When the temperature in the environment was up to 50 °C, the activity of enzymes and proteins was significantly inhibited, eventually leading to cell death. The antibacterial activities of GO, GO-Tob and GO-Tob@CuS nanoplatforms were further evaluated through live/death experiments. After being treated with GO and GO-Tob, a number of bacteria were dead, which was displayed as red fluorescence. Under NIR laser irradiation, all bacterial cells died after processing by the GO-Tob@CuS nanoplatform (Fig. 2(b)). The morphological study of bacteria by scanning electron microscopy (SEM) showed that the untreated *P. aeruginosa* and *S. aureus* were typically round and rod-shaped, respectively. After treatment with GO and GO-Tob under NIR lasers (980 nm, 1.5 W cm^{-2}), the shape of most living cells remained unchanged. However, under NIR laser irradiation, after GO-Tob@CuS treatment, all bacterial cells were destroyed and wrinkled, indicating that they were eradicated (Fig. 2(c)). These results showed that GO-Tob@CuS could

irreversibly destroy bacterial membranes through nanoknives, enhancing PTT and PDT effects, and leading to bacterial death.

The success of graphene nanomaterials has laid a reliable foundation for nanoplatforms in biomedical applications. However, the application of graphene nanomaterials in biomedicine is still in its early stages and there are many challenges to overcome. The complex interaction of graphene with biological membranes causes a variety of cellular responses. For example, graphene often contaminates endotoxins during synthesis and causes septic shock, and graphene interferes with mitochondrial membrane potential to activate mitochondria-mediated apoptosis.[41] In consideration of the toxicity of graphene, a new carbon-based nanomaterial, carbon quantum dots (CDs), has been developed. CDs are novel nanomaterials for biomedical applications due to their acceptable biocompatibility, excellent water solubility, stability and luminescence properties both *in vivo* and *in vitro*. Recently, the combined use of CDs and other nanomaterials has received increasing attention, but most of the research studies were still on CD-based synergistic photothermal and photodynamic anti-tumor therapy, and very little research has been done on the use of CDs in the antibacterial field. CDs themselves have low NIR absorption and cannot meet the needs of phototherapy. Therefore, the development of new NIR-emitting CDs (RCDs) for PTT and PDT is warranted. Some metal nanoparticles have excellent NIR absorption properties, but their toxicity limits their biomedical application. Considering these two points, combining metal ions with RCDs can be considered to reduce the toxicity of the metal ions while enhancing the phototherapeutic effect of CDs. In addition, quaternary amino compounds (QACs) can damage cell membranes and make bacteria more sensitive to heat and ROS due to their positively charged and hydrophobic chains. Therefore, the combination of copper ions with RCDs (Cu-RCDs) and QACs (Cu-RCDs-C_{35}) achieved a tri-modal synergistic antibacterial treatment with photothermal, photodynamic and quaternary ammonium salts. In this study, Cu-RCDs were obtained by combining Cu^{2+} with RCDs *via* N–Cu–N. The QACs (cocoamidopropyl betaine, CAB-35) were then combined with Cu-RCDs *via* a carboxamide reaction to give Cu-RCDs-C_{35} (Fig. 2(d)).[42] Cu-RCDs-C_{35} exhibited some more satisfactory features than other CD-based nanomaterials: (1) the tri-modal synergistic antibacterial effect of Cu-RCDs-C_{35} was better for both Gram-positive and Gram-negative bacteria; and (2) the synergistic effect at lower ROS concentrations and temperatures promoted wound healing and avoided inflammatory reactions. The temperature of Cu-RCDs-C_{35} (800 μg mL^{-1}) under 808 nm light irradiation quickly increased to 57.3 °C and the photothermal conversion efficiency (PCE) of Cu-RCDs-C_{35} was 32.47%, which was slightly higher than that of RCDs-C_{35} (29.51%), indicating that the doping of Cu^{2+} enhanced the photothermal therapeutic effect of RCDs-C_{35}. The 1,3-diphenylisobenzofuran (DPBF) experimental results showed that Cu-RCDs-C_{35} could efficiently produce ROS under NIR light irradiation at 808 nm and that the N–Cu–N structure was the key. Even after treatment with 800 μg mL^{-1} of Cu-RCDs-C_{35}, the cell survival rate was still 85%, which can prove that the biocompatibility of Cu-RCDs-C_{35} is satisfactory. In the absence of light, the antibacterial effect of Cu-RCDs and Cu-RCDs-C_{35} increased with increasing concentrations. The antibacterial activity of both compounds at a concentration of 800 μg mL^{-1} was 35.2% and 62% for *Escherichia coli* (*E. coli*) and 35% and 66% for *S. aureus*, respectively. The enhancement of antibacterial activity was attributed to the disturbance of the cell membrane by QACs. The RCDs-C_{35} + laser group showed 80% and 82% antibacterial rates against *E. coli* and *S. aureus*, respectively, reflecting the synergistic antibacterial effect of PTT and quaternary ammonium salts. The Cu-RCDs-C_{35} + laser group demonstrated the highest antibacterial efficiency, which was 99.36% and 99.98% for *E. coli* and *S. aureus*, respectively, attributed to the synergistic antibacterial effect of quaternary ammonium salts, PTT and PDT. The above experimental results showed that Cu-RCDs-C_{35} had the highest antibacterial efficiency under NIR light irradiation at 808 nm through the tri-modal synergistic antibacterial treatment of photothermal, photodynamic and quaternary ammonium salts (Fig. 2(e)). Encouraged by the efficient *in vitro* antibacterial efficiency of Cu-RCDs-C_{35}, the therapeutic efficiency and wound healing process of light-mediated Cu-RCDs-C_{35} for infected wounds were evaluated. Photographs of the wounds of the different experimental groups on days 1, 3, 7, 10 and 14 are shown in (Fig. 2(f)). All groups were inoculated with *S. aureus* on the first day, giving the wounds the same degree of infection. On day 3, the degree of infection was reduced in all groups except the PBS + laser group. After 7 days, the infected areas began to crust and the crusts gradually darkened in the group that received NIR light. The crusts then slowly fell off in the Cu-RCDs-C_{35} + laser group, while this did not occur in the other test groups. After 14 days, the crusts disappeared and the Cu-RCDs-C_{35} + laser group had the best wound healing effect, indicating that the Cu-RCDs-C_{35} + laser group had a better effect on promoting wound healing compared to the other groups. Therefore, the photothermal antibacterial properties of CDs with high biocompatibility can be improved by doping metal ions, which will contribute to the development of carbon-based nanoplatforms as antibacterial materials with considerable potential in the biomedical field.

Noble metals, such as gold, silver and palladium are usually considered as photothermal antibacterial agents owing to their excellent ability to convert light energy into thermal energy.[43] Some researchers have confirmed that the shapes of noble metal materials have a large influence on their photothermal effects. For example, gold nanorods (Au NRs) have the highest PCE among many gold nanocrystals with other shapes, and can be applied in PTAT to kill bacteria. However, in the preparation of Au NRs, cetyltrimethylammonium bromide (CTAB) is essential to improve the stability. CTAB is a cationic surfactant, but it has low compatibility and high toxicity for molecular biofilms. So, it is necessary to remove CTAB from the surface of Au NRs or replace it. The coating of Au NRs by mesoporous silica can reduce the toxicity of surface CTAB and provide an opportunity for drug loading. Curcumin (Cur) is a polyphenolic substance derived from the rhizomes of Araceae. Cur not only has a variety of pharmacological activities, but also serves as a

photosensitizer with antibacterial photodynamic potential. However, its poor water solubility, structure instability, low bacterial affinity, and rapid elimination *in vivo* limit its application in the therapeutic field. To overcome these shortcomings and improve the efficiency and stability of photosensitizers, Cur is usually loaded on small molecules or macromolecule carriers to form nanoagents. Based on this, Zhang *et al.* selected mesoporous silica modified Au NRs as carriers to load Cur and constructed a multi-functional composite antibacterial nanosystem (AuNRs@Cur) with dual PTT and PDT antibacterial effects.[44] Compared with pure Cur and AuNRs, AuNRs@Cur had a higher single-line oxygen yield efficiency and PCE, which greatly improved the utilization rate of photosensitizers and effectively enhanced the photoinactivation effect. Under 808 nm irradiation, the antibacterial effect of Cur (90%) was weaker than that of AuNRs@Cur (100%) at a concentration of 0.001 μM. Under dual exposures of 405 nm and 808 nm, antibacterial effect with AuNRs@Cur was higher than that of Cur or AuNRs alone. The results further verified that the reactive oxygen and thermal energy produced by double wavelength (405 + 808 nm) laser irradiation can kill bacteria synergistically by destroying the bacterial outer membrane structure and cause bacterial death. Moreover, AuNRs@Cur's cytotoxicity and hemolytic activity were insignificant, indicating that AuNRs@Cur could significantly reduce the toxicity of Cur to normal human hepatocytes and increase the biocompatibility of nanocarriers. Bisides the mentioned mesoporous silica, metal sulfides are also frequently used for hybridization with Au NRs. Previous studies revealed that light-sensitive materials can also produce a large number of electron hole pairs under irradiation of light with a specific wavelength, resulting in the production of $^{\bullet}OH$, $^{1}O_2$ or $^{\bullet}O^{2-}$.[45] Bi_2S_3, as an n-type semiconductor with satisfactory absorption ability, is widely regarded as an excellent PTA and photocatalyst with good biocompatibility and is widely concerned in the antibacterial field. Here, Wang *et al.* prepared sea urchin-shaped Au@Bi_2S_3 core–shell structures through an intermediate layer transformation strategy. This structure has good biocompatibility and excellent PCE *via* a hard template combined with polyol.[46] The poor photothermal stability of the Au NRs themselves was also improved by coating sulfides. Importantly, this metal–semiconductor composite nanostructure can be seen as a typical Schottky junction, which can improve the separation efficiency of electron–hole pairs triggered by NIR light, leading to a high production of ROS. Therefore, the sea urchin-like Au@Bi_2S_3 core–shell structures could achieve rapid inactivation of Gram-negative bacteria (*E. coli*) and Gram-positive bacteria (*S. aureus*) triggered by NIR light compared to Au NRs or Bi_2S_3 NPs alone owing to their synergetic photothermal and photodynamic antibacterial performance.

Although noble metal nanoparticles as PTAs show excellent antibacterial performance, they are limited by their inherent characteristics, such as poor biocompatibility, high cost, poor photostability, cumbersome preparation process, and low targeting efficiency for bacteria. Noble metal nanoparticles tend to accumulate in colloidal solutions due to their high surface energy, resulting in the low release of metal ions, thus reducing antibacterial activity, especially in the *in vivo* environment.[47] Semiconductor nanomaterials (metal sulfides, metal oxides, *etc.*) as a new type of PTT and PDT material have the advantages of low cost, NIR laser triggering and high stability.[48] Currently, molybdenum disulfide (MoS_2) has received increasing attention as a phototherapy nanocarrier due to its easy synthesis, high NIR absorption performance and good biocompatibility. Therefore, MoS_2 can rationally integrate with other nanomaterials in order to achieve the goal of improving antibacterial efficiency. Recently, Li *et al.* developed a photothermally activated antibacterial nanoplatform consisting of MoS_2 nanosheets, ICG photosensitizers, and Ag nanoparticles (MoS_2/ICG/Ag) (Fig. 3(a)).[49] As shown in Fig. 3(b), MoS_2/ICG/Ag with excellent NIR absorbing ability has more sufficient photothermal properties than part of them used alone. Subsequently, DPBF acts as a $^{1}O_2$ indicator to detect the $^{1}O_2$ generation of MoS_2/ICG/Ag. In the same way, as shown in Fig. 3(c), MoS_2/ICG/Ag displayed a higher SOSG fluorescence intensity than MoS_2/ICG under the same conditions because the doping of Ag nanoparticles. Ag^+ ions can be oxidized from Ag nanoparticles in aqueous solutions; this process can be further enhanced by hyperpyrexia. After irradiation with an 808 nm laser for 30 min, the amount of Ag^+ released from MoS_2/ICG/Ag reached 43.4%, which was higher than that of the control group (13.3%) without light irradiation (Fig. 3(d)). This result indicated that hyperpyrexia accelerated the release of Ag^+ from MoS_2/ICG/Ag and the released Ag^+ could produce ROS to improve antibacterial efficiency. Briefly, the photonic hyperthermia generated by MoS_2 accelerated the release of ICG and silver ions; this result could in turn improve the performance of PTT, which was a mutually reinforcing effect that could produce a combined or even synergistic therapeutic effect. The *in vitro* bactericidal effect of MoS_2/ICG/Ag under 808 nm NIR laser irradiation was evaluated using the plate count method. *S. aureus* and *E. coli* were used as models for Gram-positive and Gram-negative bacteria in a broad-spectrum antibacterial assay. Treatment of *S. aureus* with MoS_2 + NIR, ICG + NIR and MoS_2/ICG + NIR resulted in bacterial survival rates of 59.5%, 69.4% and 20.0%, respectively. Similarly, those of *E. coli* in the MoS_2 + NIR and ICG + NIR groups reached 58.5%, 72.8% and 22.5% respectively. These results suggested that the combination of PTT and PDT had a better antimicrobial effect than PTT or PDT alone, but the combined PTT/PDT treatment does not completely eliminate the bacteria. Notably, for the PTT/PDT/chemotherapy tri-modal treatment group of MoS_2/ICG/Ag + NIR, the survival rates of both *S. aureus* and *E. coli* were close to zero, indicating that MoS_2/ICG/Ag had the best broad-spectrum antibacterial activity under NIR light irradiation at 808 nm. The experimental protocol for *in vivo* antimicrobial membrane treatment in animals is shown in Fig. 3(e). Mice infected with the biofilm were divided equally into PBS, MoS_2, MoS_2/ICG, MoS_2/ICG/Ag, MoS_2 + NIR, MoS_2/ICG + NIR and MoS_2/ICG/Ag + NIR groups. As shown in Fig. 3(f), the wounds of the mice in the MoS_2/ICG/Ag + NIR group healed the best, demonstrating the good antibacterial effect of MoS_2/ICG/Ag. Thus, the developed MoS_2/ICG/Ag triple bactericidal system (including PTT, PDT and

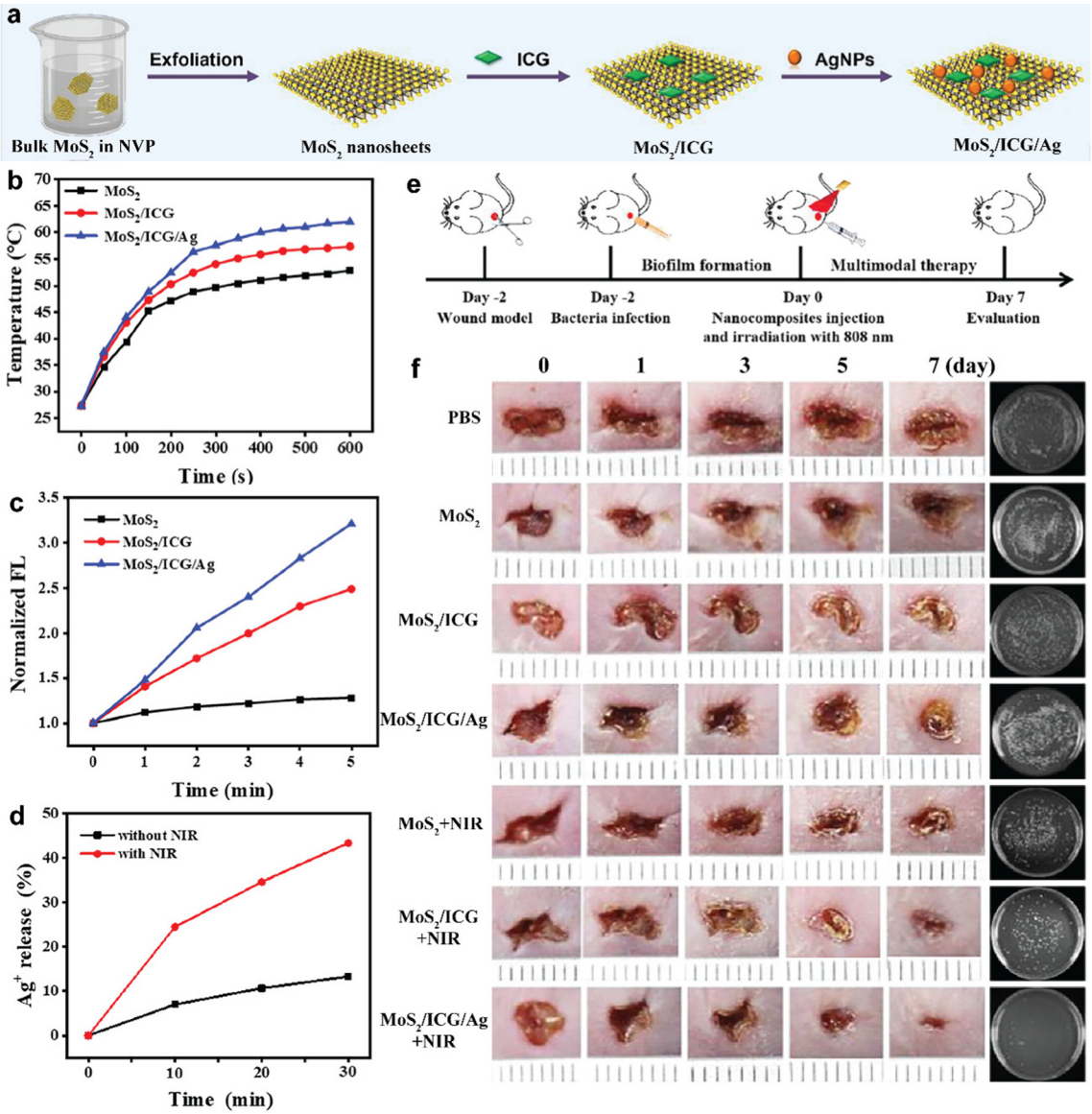

Fig. 3 (a) Schematic illustration of the preparation of multifunctional MoS_2/ICG/Ag nanocomposites. (b) Photothermal curves of MoS_2, MoS_2/ICG, and MoS_2/ICG/Ag with 808 nm laser irradiation (1.0 W cm^{-2}). (c) Comparison of SOSG fluorescence intensities in the presence of different nanocomposites with irradiation with an 808 nm laser (1.0 W cm^{-2}) for 5 min. (d) Controlled release profiles of Ag^+ from MoS_2/ICG/Ag (150 μg mL^{-1}) with (red line) and without (black line) 808 nm laser irradiation (1.0 W cm^{-2}) for 10 min. (e) Schematic illustration for the establishment of an *in vivo* biofilm-infected wound model and the subsequent treatment regime. (f) Digital photos of *S. aureus* biofilm-infected wounds. Reprinted with permission of ref. 49. Copyright 2022 Elsevier.

chemotherapy) showed a good synergistic effect in inhibiting biofilm formation and killing deep biofilm bacterial cells. This study will provide a theoretical basis for the application of light-induced multifunctional platforms in killing bacteria and fighting complex biofilm infections.

Copper, as the main biologically active component of the human body, is an essential trace element with a special biological role. Cu-based nanomaterials have become a hot spot in NIR-induced bactericidal research. Among them, copper sulfide nanoparticles (CuSNPs), as a new class of PTT and PDT materials were used for their low cost, triggering by a 980 nm laser, and high photostability.[50] To improve the hydrophilic and targeted bacterial ability of CuSNPs, Dai *et al.* constructed a collection of poly(5-(2-ethyl acrylate)-4-methylthiazole-*g*-butyl)/copper sulfide nanoclusters (PATA-C4@CuS), which was composed of thiazole derivatives with a quaternary ammonium salt (PATA-C4) and CuSNPs.[51] In PATA-C4, the thiazole ring could make the enzymes and proteins in bacteria inactive, so it possesses prominent antibacterial activity against a wide spectrum of antibiotic-resistant bacteria. A quaternary ammonium salt as a cationic antimicrobial molecule can also be added to this nanoplatform; its positive charges can interact with negatively charged bacteria through electrostatic interaction and damage the membrane of bacteria. Hence, NIR laser

irradiation could make bacteria aggregate and then improve antibacterial efficiency. The *in vitro* antibacterial results confirmed that PATA-C4@CuS with PTT, PDT, and membrane-targeted ligands had satisfactory antibacterial effect. In recent years, defect engineering has been considered an applicable strategy for enhancing photocatalytic activity. The sulfur vacancies (V_s) of some metal sulfides have attracted much attention due to their ability to promote the redshift of the absorbed light, enhance the utilization of light energy, and increase photocatalytic bactericidal activity.[52] Based on this point, Mo *et al.* constructed various CuS nanosheets with V_s by the hydrothermal synthesis method.[53] Without NIR light, the CuS nanosheets did not show a significant effect on the survival of *E. coli* and *Bacillus subtilis*, which indicated that the CuS material itself had no significant effect on the bactericidal efficiency. However, under 808 nm laser irradiation, the viability of the bacteria dramatically decreased. Importantly, CuS nanosheet (CuS-3) with more V_s and a narrower band gap, which was favorable for enhanced light absorption and electron transfer efficiency, had the highest PCE and ROS level. The strong local thermal effect and a large amount of ROS under NIR irradiation could cause oxidative damage to the bacteria. Therefore, compared to other CuS nanosheets, the CuS-3 group exhibited significant bactericidal properties in synergy with PDT and PTT. This study will contribute to the design of synergistic photothermal–photodynamic antibacterial agents for efficiently killing bacteria with abundant V_s based on the structure–activity relationship.

Mussel-inspired polydopamine (PDA) has attracted growing attention in sensing applications because it combines biocompatibility and unique adhesive properties. With facile preparation methods based on self-polymerization, it has the potential to be developed into simple, rapid, and economical nanoparticle platforms.[54] Recent investigations demonstrated that PDA could efficiently convert NIR light into heat and kill bacteria and cancer cells *in vitro* and *in vivo*. To realize rapid and effective antibacterial treatment, a PAM–PDA/Ag@AgCl hydrogel with synergistic local PTT and PDT was designed and constructed.[55] First, the PAM–PDA hydrogel was prepared *via* noncovalent interactions of PDA chains and polyacrylamide (PAM) networks. Second, Ag^+ and Cl^- was combined in Tris-HCl buffer solution through ionic interaction to form AgCl. Meanwhile, partially AgCl was reduced to Ag through reduction by catechol groups in the PDA chains, to form Ag@AgCl in the hydrogel. This PAM–PDA/Ag@AgCl hydrogel showed excellent photothermal properties, which was attributed to the combination with PDA. The electron spin resonance spectra showed the generation of $^1O_2$ and $^\bullet OH$ from Ag@AgCl nanostructures in the hydrogel. Because NIR can trigger PTT and PDT simultaneously, synergistic local PTAT and PDAT with fewer side effects was expected to be achieved. For *E. coli* and *S. aureus*, under NIR light irradiation for 10 min the PAM–PDA/Ag@AgCl hydrogel had a fast and effective antibacterial effect (99.91 and 99.97%), while a single PTT (50%) or PDT (70%) could only provide a moderate antibacterial effect. Therefore, PAM–PDA/Ag@AgCl had significant antibacterial effect at a relatively low temperature (52.1 °C) and moderate the production of ROS. This PTT and PDT effectively improved the permeability of bacterial membranes. After the rupture of the bacterial membrane, oxidative stress and serious protein leakage could lead to bacterial death. Importantly, due to the negligible side effects, this system has great clinical potential for sterilization through the combination of PTT and PDT.

Porphyrin is a class of macromolecular heterocyclic compounds formed by the interconnection of α-carbon atoms of four pyrrole subunits through sub-methyl bridges (=CH–).[56] The porphyrin ring has twenty-six π electrons, which is a highly conjugated system. The porphyrin compounds containing heavy atoms, cations and appropriate substituents are widely used in antibacterial PDT because of their high reactive oxygen yield, good affinity with bacterial membranes, and non-stacking properties. Hu *et al.* designed and synthesized a water-soluble cationic porphyrin, 5,10,15,20-tetrakis-(4-*N*-methylpyridyl)-porphyrin (TMPyP), with an iodine anion as an anion.[57] TMPyP carried four positive charges on the peripheral *N*-methylpyridine group, which enhanced the water solubility of hydrophobic porphyrin rings and helped adsorb by negatively charged bacteria. However, as a small molecule with a positive charge, TMPyP could destroy cell membranes and cause cell death, so it was highly cytotoxic to intestinal cells. In order to reduce cytotoxicity, the host–object complex was formed between TMPyP and cucurbit-[7]uril (CB[7]) by the supramolecular method. The reduction reaction of supramolecular porphyrin TMPyP/$(CB[7])_4$ to bacteria was almost the same as that of the original TMPyP, indicating that the porphyrin core was not shielded by the host–object interaction. In addition, the peripheral electron suction substituent of TMPyP promoted the reduction of porphyrin centers, while the substituents were not directly involved in electron capture. In a hypoxic environment, TMPyP could be reduced to phlorin by some facultative anaerobic bacteria with strong reduction ability, such as *E. coli* and *Salmonella* typhoid in mice. It had strong NIR absorption and significant photothermal conversion ability, and showed good antibacterial activity through PTT. In an aerobic environment where aerobic bacteria such as *Bacillus subtilis* and *P. aeruginosa* did not reduce, TMPyP was a typical photosensitizer that could effectively kill bacteria through PDT. However, porphyrins could only have PTT antibacterial effects on some facultative anaerobic bacteria and PDT antibacterial effect on aerobic bacteria, so porphyrins did not play PTT–PDT collaborative antibacterial. Thus, in one environment and at the same time, the porphyrin compound playing to the synergistic PTT–PDT antibacterial effect will be conducive to improving the antibacterial effect and reducing the side effects of a single treatment. Sun *et al.* synthesized porphyrin-based covalent organic frameworks (COFs) and combined them with PTT and PDT to achieve enhanced antibacterial effects.[58] COF is a highly crystalline functional porous carbon-based material composed of light atoms (such as carbon, nitrogen, oxygen and borane), which shows potential application prospects in the field of biomedicine. Porphyrin-based COF nanosheets (TP-Por CON) were constructed for combined PDT and PTT treatment under red

light (for example, 635 nm). The porphyrin-based porous COF was prepared by an esterification reaction between 5,15-bis(4-boronopHenyl)-porphyrin and 2,3,6,7,10,11-triphenylenehexol (HHTP) (Fig. 4(a)). Subsequently, TP-Por COF was added to PBS and ultrasonic processing was carried out to obtain high-quality small-layer TP-Por CON. In addition, the NO donor molecule BNN6 was wrapped in the pore of the crystal porous skeleton structure (TP-Por CON@BNN6), and NO was moderately released under red light to realize NO treatment. As shown in Fig. 4(b), TP-Por CON@BNN6 catalyzed water and oxygen molecules to $^{\bullet}OH$ and $^{\bullet}O^{2-}$. Excessive ROS not only seriously undermined the balance of GSH/GSSG levels and led to oxidative stress, but also induced lipid and DNA peroxidation. Some proteins, such as heat shock protein, were inhibited by ROS to amplify the effect of PTT. The permeability and integrity of the plasma membrane had begun to be destroyed at this moment. Continuous light irradiation, plasma membrane rupture, and intracellular protein degeneration, which were due to the high temperature caused by TP-Por CON@BNN6, promoted the apoptosis of bacterial cells. During this period, when BNN6 molecules received red light and thermal energy, NO free radicals were released. In the presence of $^{\bullet}OH$, NO can be oxidized to peroxynitrite ($ONOO^{-}$) and nitrous trioxide (N_2O_3). These additional reactive nitrogen species (RNS) produced by NO could further improve plasma membrane permeability, damage bacterial cell membranes, and significantly damage DNA, making bacterial cells more vulnerable and sensitive to heat. In the final stage, the bacterial cell wall and plasma membrane were completely destroyed, and bacterial cell contents such as potassium/sodium ions, plasmid DNA, RNA and proteins flowed out of cells. This antibacterial chain reaction caused by a single visible light source was a three-ray strategy, which did not lead to bacterial resistance. The photothermal conversion capacity of the TP-Por CON carrier was studied, and the TP-Por CON@BNN6 water suspension was placed for 6 min under red light (635 nm, 1 W cm^{-2}). It was calculated that the PCE (η) of TP-Por CON@BNN6 had reached 18.4%, which proved the effectiveness of converting photoirradiation into thermal energy. Impressively, once the 635 nm laser was turned on, a significant increase in NO release had been observed at different points in time, indicating that NO concentrations were highly dependent on radiation throughout the study time. Research on the photosensitivity characteristics of TP-Por CON@BNN6 showed that TP-Por CON@BNN6 could effectively produce $^{\bullet}OH$ and $^{\bullet}O^{2-}$ to attack bacterial cells under 635 nm laser exposure. The results of the *in vitro* antibacterial test showed that TP-Por CON@BNN6 integrated heterojunction could well combine the advantages of PDT, PTT and gas therapy (GT), and showed good antibacterial activity *in vitro*. Moreover, TP-Por CON@BNN6 had good biocompatibility and negligible cytotoxicity, and the toxicity of light irradiation was negligible. One possible reason for the difference in cytotoxicity between eukaryotic cells and prokaryotic cells was the different cell structures, autophagy and lysosome degradation in eukaryotic cells. As shown in Fig. 4c representative wound images of control and PDT, PTT + PTT and PTT + PTT + GT processed mice at different points in time. Quantitative data curves are shown in Fig. 4(d). On day 1, TP-Por CON@BNN6 would be irradiated with red light (1.0 W cm^{-2}) for 10 min. On day 3, mice injecting PBS (control group) accumulated pus in the damaged wound, while no pus was seen in the PTT + PTT + GT group, PTT + PTT group and PTT group. On day 5, the wound area generally became smaller, and scars appeared in all three treatment groups except the control group. On day 7, the skin injury area of mice in the PTT + PTT + GT group recovered significantly (the corresponding wound healing rate was 78%), showing the trend of effective wound healing in this group, while the wound area of other groups still reached 71%, 48% and 47%, respectively. On day 7, the degree of wound inflammation and swelling in the PDT + PTT group was significantly higher than that in the PTT + PTT + GT group. On day 12, although the wounds in all groups were almost completely closed, there were some differences between the treatment groups. It is worth noting that the wounds of mice treated with PBS, PTT and PTT + PTT were scabbed, while the wounds of mice treated with PDT + PTT + GT were not scabbed, indicating that good synergy promoted the healing of chronic infection wounds. The antibacterial effect of TP-Por CON@BNN6 *in vivo* was detected by the plate method. The lowest number of colonies of the PDT + PTT + GT group showed that the NO-release nanodrug could be used to eradicate *S. aureus in vivo* (Fig. 4(e)). The study of intracellular inflammatory cytokines and the level of repair of cytokines through immunofluorescence staining showed that PDT + PTT + GT could effectively inhibit early inflammatory response (Fig. 4(f)). It was then confirmed that the combined application of PDT + PTT + GT could increase the expression of α-SMA and CD31 (Fig. 4(g) and (h)), suggesting that these repair cytokines effectively promoted the formation of collagen fibers and neovascularization. TP-Por CON@BNN6 integrated heterojunction triple antibacterial model, good biocompatibility and multifunctional biological activity is an attractive treatment method that can destroy the development of bacterial drug resistance and is a method with future biological application prospects.

Once the skin is seriously traumatized or damaged by burns, open wounds are susceptible to bacterial infections, and wound dressings are usually needed to fight bacteria. Hydrogel has attracted much attention due to its interconnected microporous network, which can maintain a humid microenvironment and promote the absorption of wound exudate and the transmission of oxygen. Ran *et al.* designed and synthesized an injectable hydrogel for real-time bacterial detection, efficient bacterial capture and disinfection, and on-demand removal of bacterial fragments to promote the healing of infected wounds.[59] PDA nanoparticles have attracted more and more attention because of their biocompatibility and biodegradability, while ε-polysine (ePL) is a typical antibacterial peptide with rich L-lysine residues, which produces a broad spectrum of antibacterial activity by destroying bacterial walls. ePLU was obtained as a supramolecular self-assembly group by bonding hexamethylene diisocyanate (HDI) on ePL, and the obtained

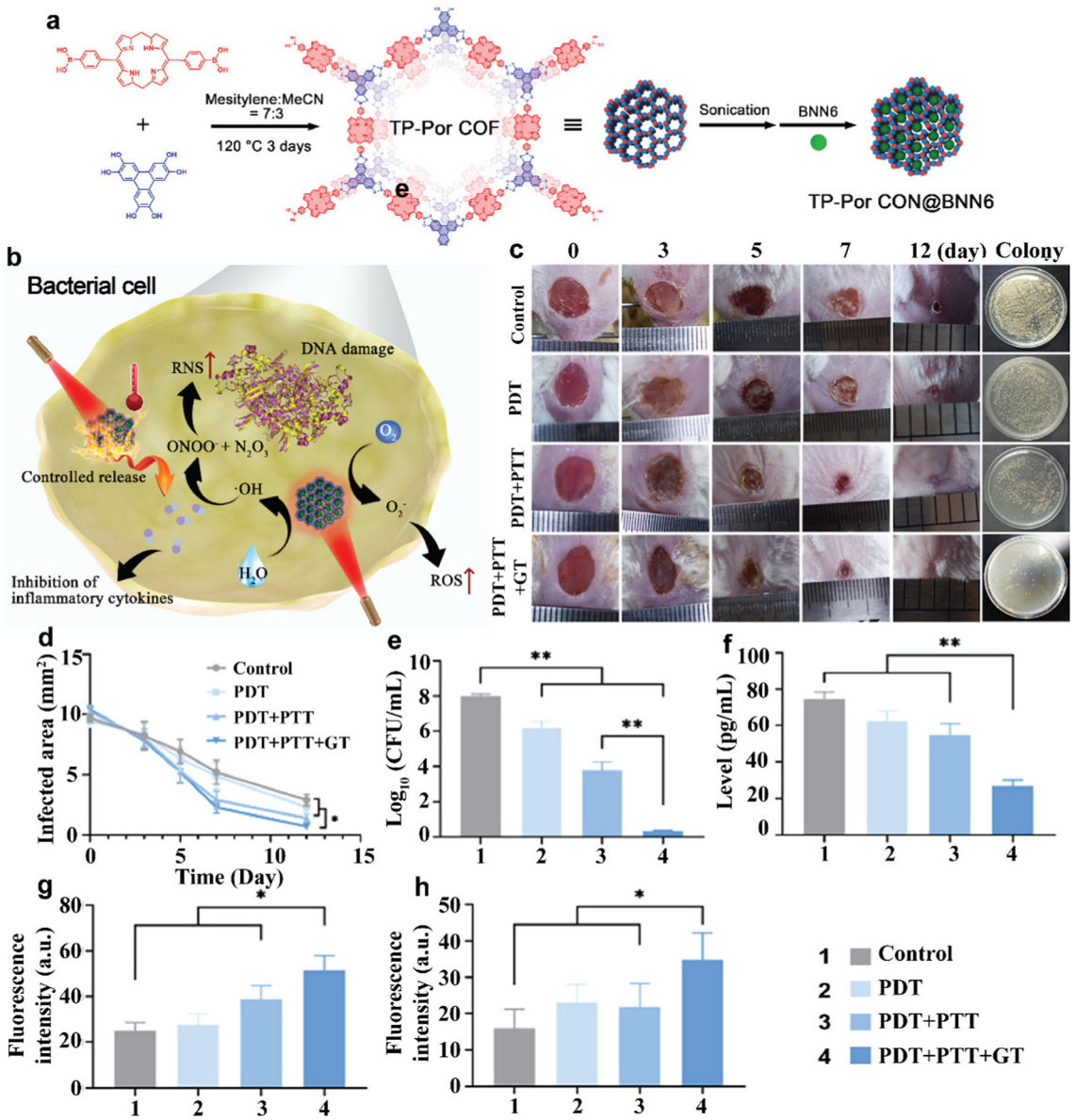

Fig. 4 (a) Schematic illustration of the synthesis of TP-Por CON@BNN6. (b) TP-Por CON@BNN6-integrated heterojunction destroyed the bacterial cells by producing ROS, increasing the temperature, and releasing NO, realizing a synergistic effect of PDT, PTT, and GT. *In vivo* antibacterial activity and *S. aureus*-infected chronic wound healing receiving different treatments (PBS, PDT, PDT + PTT, and PDT + PTT + GT). (c) Representative photographs of the chronic wound with different treatments at 0, 3, 5, 7, and 12 days and the images of *S. aureus* colonies grown on the agar plates derived from the homogenized infected tissues after various treatments for 12 days. (d) The quantitative analysis of the residual wounded areas. (e) The quantitative analysis of the bacterial colony-forming units obtained from different tissues of mice. (f)–(h) The quantitative analysis of the fluorescence intensity for TNF-α, α-SMA, and CD31. Significance was assessed using Student's *t* test, giving *P* values, $^{*}P < 0.05$, $^{**}P < 0.01$. NS, no significant difference. Reprinted with permission of ref. 58. Copyright 2021 American Chemical Society.

ePLU hydrogel crosslinked through a well-defined quadruple hydrogen bond. Tetrakis(4-carboxyphenyl)-porphyrin (TCPP) photosensitive agent was loaded on PDA nanoparticles by π–π accumulation and PTC nanoparticles were obtained, and PLU@PTC hydrogel was prepared by crosslinking the benzoquinone group of PDA with the amino group of ePLU. Therefore, the ePLU injection solution containing PTC nanoparticles could be connected to *in situ* induce sol–gel transformation through hydrogen bonds and Schiff base. PDA nanoparticles with the melanin structure could quench out the fluorescence emission of TCPP, and the release of TCPP triggered by the acidic microenvironment of bacterial infection could restore fluorescence emission, which was used for real-time imaging of infected wounds under 410 nm light. Then, TCPP released from infected wounds was irradiated at 660 nm to initiate accurate antibacterial PDT therapy. Bacteriological capture on hydrogel strengthened this effect and alleviated the limitation of the short distance of ROS. Under 808 nm of light, the hydrogel wrapped in bacterial fragments was removed, and the change of hydrogel dressing accelerated the healing of infected wounds

by simultaneously reducing oxidative stress, regulating inflammatory factors, accelerating collagen deposition and promoting angiogenesis. Hydrogel dressing paves a new way for the development of a fine and simple treatment platform for bacterial infections and chronic wound treatment.

2.2 Synergistic chemo-photothermal antibacterial therapy

Antibacterial chemotherapy refers to the use of chemical drugs (such as antibiotics, metal ions, *etc.*) to prevent bacterial proliferation and wound infection. Preventing the spread of an existing local infection by using various antibiotics plays an essential role in lowering the risk of further deterioration. However, nearly 80% of multidrug-resistant or extremely drug-resistant microorganisms have arisen due to the global overuse or misuse of antibiotics, and infection by these strains is accompanied by severe adverse effects such as thrombophlebitis and epidermal necrolysis. To achieve the goal of timely infection control, it is essential to develop novel antimicrobial approaches that can treat infections with a minimal antibiotic dose. Recently, photothermal conversion capabilities of nanoparticles such as gold nanoparticles, iron oxide, graphene, black phosphorus, and other polymer nanoparticles have been designed to intelligently deliver antibiotics to infected sites for chem-photothermal therapy under NIR irradiation. Synergetic chemo-photothermal antibacterial therapy can give full play to the advantages of both and enhance the antibacterial effect, as well as reduce the side effects caused by external NIR irradiation, thermal damage, and high dose of antibiotics.

Temperature-responsive nanostructures (TRN) have a large melting latent heat and reversible solid–liquid transformation in a narrow temperature range than other nanoplatforms; this can realize accurate drug release.[60] Due to the advantages of convenient assembly, excellent chemical stability and low toxicity, TRN has achieved great success in tumor treatment. It is believed that TRN can be used as a nanocarrier for effective antibacterial treatment. There are a few characteristics of TRN: (1) satisfactory biocompatibility and it can completely encapsulate antibiotics without leakage; (2) it is easy to combine several nanomaterials in a nanoplatform; (3) under NIR, antibiotics encapsulated can be released more quickly; and (4) it can combine antibacterial activity of PTT with antibiotics. Consider the advantages of TRN, Qing *et al.* developed a thermo-responsive-inspirated drug-delivery nano-transporter for the synergistic eradication of multidrug-resistant bacteria (Fig. 5(a)). Lauric acid and stearic acid were utilized to prepare TRN, and then imipenem (IMP, a broad-spectrum antibiotic) and IR780 (a photosensitizer molecule) were encapsulated into TRN. Finally, phospholipids were used to wrap the drug-loaded TRN and form IMP/IR780@TRN nanospheres. In IMP/IR780@TRN, fluorescent IR780 molecules can realize real-time monitoring of the release of IMP/IR780@TRN at the infection site possible; this can help us choose a suitable time to turn on NIR laser. In addition, thermal response generated by NIR-irradiated IR780 molecules not only make TRN melted, but also damage the membrane of bacteria, which accelerated the third effect that decreased IMP's resistance and made IMP penetrate into the membrane faster; this could interfere the formation of cell wall chemically. The results of standard plate counting showed that the colonies of antibiotic-sensitive *E. coli* and *S. aureus* treated with IR780@TRN and 3× IMP (three times the dosage of that in IMP/IR780@TRN) were reduced by 40–50%, but the IMP treatment group based on the theoretical release had negligible antibacterial effect, indicating that PTT or high doses of IMP alone used in this study had moderate antibacterial effect. However, NIR-irradiated IMP/IR780@TRN could effectively kill both bacteria, it can be seen from the result of standard plate counting experiment. Most IMP/IR780@TRN could maintain at the infected area and this process can last 48 h. Moreover, at the end of irradiation the average temperature of the infected area was increased to 49 °C,

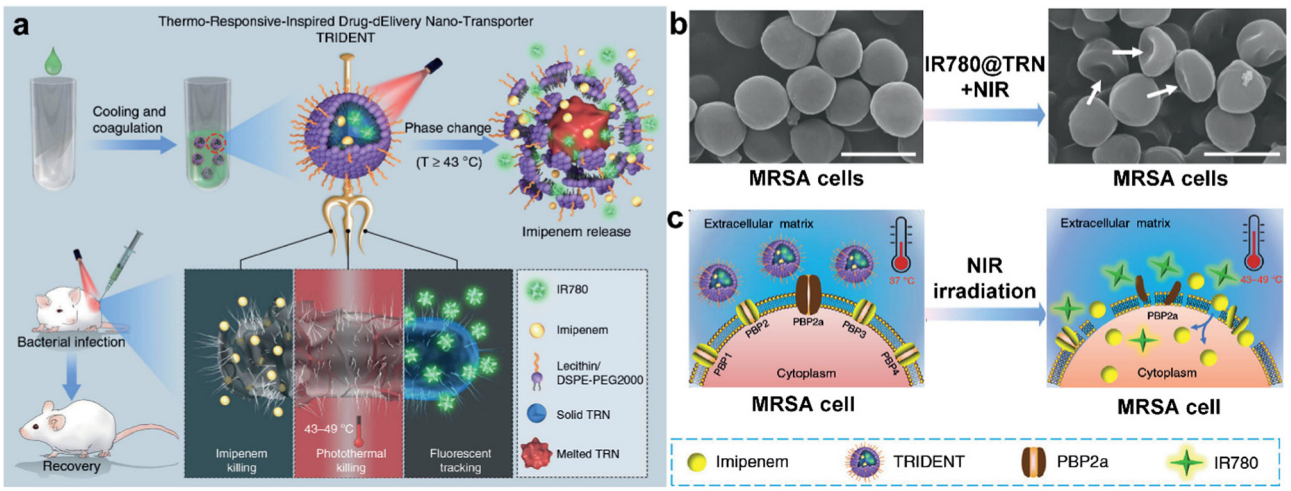

Fig. 5 (a) The prepared thermo-responsive-inspired drug-delivery nanotransporter (IMP/IR780@TRN) "melts" when the temperature increases above 43 °C under NIR irradiation, leading to the release of imipenem to the infected site. (b) SEM images of bacteria (MRSA cells) before and after treatment by IR780@TRN + NIR. Scale bars: 1 μm. (c) Scheme of the killing process on MRSA by IMP/IR780@TRN under NIR irradiation. Reprinted with permission of ref. 60. Copyright 2019 Springer Nature.

which would not only promote PTT, but also activate the injected IMP/IR780@TRN while decreasing the negative influence generated from hyperthermia. Methicillin-resistant *S. aureus* (MRSA) is resistant to β-lactam antibiotics because of its *mecA* gene, which encodes an additional penicillin-binding protein 2a and blocks the action of β-lactam antibiotics. In IMP/IR780@TRN, heat generated under NIR participated in the lysis of MRSA by inactivating the proteins/enzymes in bacteria membrane and damage membrane (Fig. 5(b)). IMP could penetrate into the damaged structures more easily, and then lead to MRSA death (Fig. 5(c)).

Therefore, encapsulation of the antibiotic and photosensitizer into a TRN has potential for further development into a clinical agent to fight against multidrug-resistant or extremely drug-resistant bacteria.

A previous study reported that bacteria can assume L-shaped forms to escape attack by β-lactam antibiotics.[61] L-forms are cell wall-deficient variants of bacteria, which are resistant to β-lactam antibiotics and more sensitive to external physical stimulation.[62] In this regard, the use of β-lactam antibiotics to destroy bacterial cell walls before PTT is an excellent strategy, which starts with the disruption of the bacterial cell wall by amoxicillin (AMO) and is followed by PTT. Metal–organic frameworks (MOFs) have attracted substantial research efforts as a class of crystalline porous materials constructed from metal ions/clusters and organic ligands.[63,64] With a large surface area, rich compositional diversity, and structural variation, these materials hold great potential in biological fields such as a smart drug/cargo delivery platform. Zeolitic imidazolate framework-8 (ZIF-8) is an important MOF material constructed using zinc ions and imidazole ligands and has been widely used in catalysis and biomedical fields because of its easy preparation and excellent performance.[65,66] For example, ZIF-8 is stable under physiological conditions but will degrade in a mildly acidic microenvironment. This feature allows ZIF-8 to act as a pH-sensitive vehicle for drug delivery in antitumor and antibacterial applications.[67] Recently, a NIR/pH dual-stimuli-responsive nanoplatform (Pd–Cu/AMO@ZIF-8, PCAZ) based on ZIF-8, which can load antibiotic (amoxicillin, AMO) and PTAs (Pd–Cu nanoalloys, PC), has been developed (Fig. 6(a)).[68] ZIF-8 could be degraded in bacteria-infected area because of the acidic environment, and then release AMO. Following, due to the satisfactory photothermal appearance of PC nanoparticles (η as 45.8%), the nanoplatform has excellent antibacterial effect. In the *in vitro* antibacterial experiments, AMO, PC, and PCAZ were used to treat the bacterial suspensions in PBS at pH 5.5 with or without NIR laser. Because this programmatic treatment can initially destroy the membrane of the bacteria by AMO chemically and lead to bacteria death completely by PTT of PC. Under 808 nm laser irradiation, PCAZ showed the best antibacterial effect and the inhibition rates of *S. aureus* and *P. aeruginosa* reached 99.8% and 99.1%, respectively (Fig. 6(b) and (c)). It is well known that, compared to phytoplankton, more efforts need to be made to eradicate biofilms. Therefore, removing biofilms of bacteria is a decisive consideration in whether the nanoplatform can be translated into clinical application or not. The results of crystal violet staining confirmed that PCAZ completely destroyed a large number of biofilms under NIR (Fig. 6(d)). Under the same conditions of NIR, the Pd–Cu@ZIF-8 (PCZ) treatment caused 49.4% inhibition of *S. aureus* biofilm and 42.4% inhibition of *P. aeruginosa* biofilm, while PCAZ caused 75.3% and 74.8% inhibition, respectively (Fig. 6(e) and (f)). These results clearly demonstrated that PTT can efficiently remove bacterial biofilms with the assistance of chemotherapy, thereby enhancing the elimination of bacterial infections. The excellent antibacterial effect of PCAZ has also been demonstrated *in vivo*. Compared to the control group, the PCAZ group had significantly less infiltration of inflammatory cells, intact epidermis, and fewer fibrous cells, similar to normal tissue, indicating that the wound had healed. In short, the advantages of the pH/NIR dual stimuli-responsive antibacterial agents are: (1) the acidic environment of the bacterial biofilm and NIR-mediated PTT can accelerate drug release; (2) PTT-assisted chemotherapy can reduce the dose of drug and better side effect of nanoplatform, such as drug resistance; and (3) chemotherapy combined with PTT can reduce therapy time, long-time NIR may be harmful to normal cells. This promising nanoplatform has shown excellent clinical application ability for antibacterial therapy.

In the field of biofilm removal, microneedles can also effectively penetrate biofilms and transport extracellular polymer (EPS) degradation enzymes and antibacterial agents in biofilms. Compared to the use of free drugs, microneedles are able to penetrate the dense biofilm EPS barrier and transport the loaded antibacterial material into the biofilm, thus demonstrating minimal target toxicity and better antibiotic membrane effects.[69,70] Recently, Yu *et al.* designed a dissolvable microneedle patch, which destroyed the structure of the EPS matrix by enzymolysis and killed the exposed bacteria by the combination of chemotherapy and PTT.[71] Polyvinyl alcohol (PVA) was selected as the matrix for microneedle patches because of its fast dissolution speed. The levofloxacin dopamine nanoparticles (PDA@levo) wrapped in microneedles. The α-amylase-PDA@Levo microneedles were fabricated *via* a two-casting method. The microneedles are able to effectively deliver the enzymes, antibiotics, and PTAs into the membrane to improve the antibacterial effect. Under NIR, the wrapped α-amylase was released from the dissolved microneedles to degrade extracellular polysaccharides and eradicate biofilms. At the same time, levofloxacin is released in biofilms under acidic conditions and can also be accelerated under NIR irradiation. As a result, PDA@Levo nanoparticles can kill bacteria and eradicate biofilms through synergistic PTT, reducing inflammation time and promoting wound healing and tissue regeneration.

MXenes are new multifunctional two-dimensional nanomaterials composed of transition metal carbides, nitrides, and carbon nitrides. Recently, it has been observed that Ti_3C_2-MXene has a unique membrane-disruption effect. However, owing to the high surface negative charge, it is difficult to combine the nanoplatform and bacteria through electrostatic interaction. However, the antibacterial efficiency of MXenes is not so good due to low photothermal efficiency and occurrence of

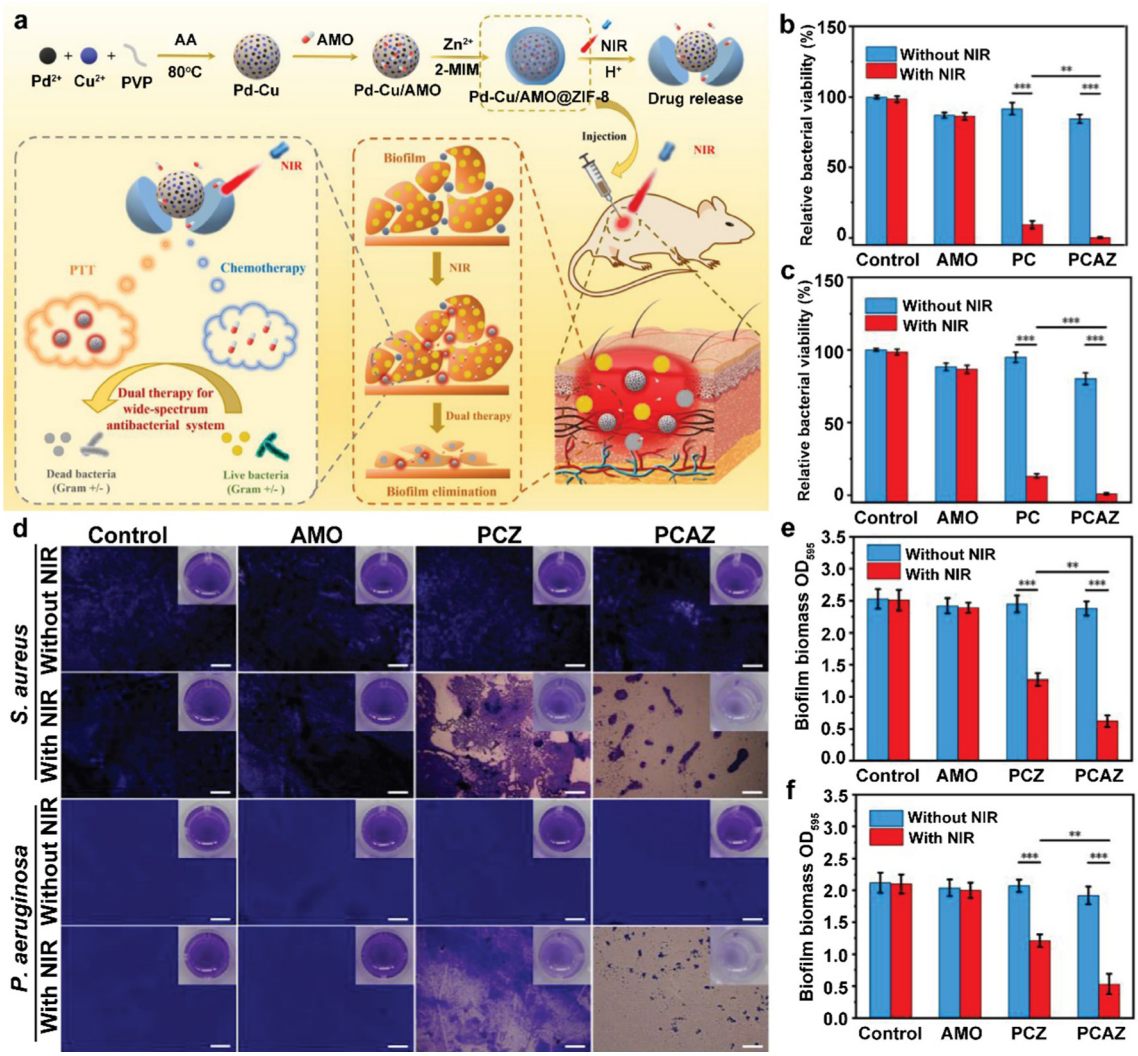

Fig. 6 (a) Schematic diagram of the dual stimuli-responsive chemo-photothermal combination system based on Pd–Cu@AMO@ZIF-8 for the procedural antibacterial therapy. Relative bacterial survival rate of *S. aureus* (b) and *P. aeruginosa* (c) after different treatments. (d) Crystal violet staining of the biofilm after different treatments (scale bars: 20 μm, inset image is the corresponding digital photograph). The statistical analysis of the relative biomass of the *S. aureus* biofilm (e) and the *P. aeruginosa* biofilm (f). Reprinted with permission of ref 68. Copyright 2022 Elsevier.

bacterial rebound *in vivo*. To enhance the antibacterial efficiency and improve selectivity of MXenes, Zheng *et al.* designed a hybrid thermo-sensitive hydrogel (Cip-Ti_3C_2 TSG) incorporated with the antibiotic ciprofloxacin (Cip) as well as nanocomposites composed of Cip and Ti_3C_2 MXene for chemo-photothermal antibacterial therapy.[72] In Cip-Ti_3C_2 TSG, the "nano knives" and PTT that led to the membrane damage could improve the penetration of Cip to achieve high-efficiency sterilization. In addition, the functionalized Ti_3C_2 nanocomposites with cationic Cip can combine with the bacteria membrane through electrostatic interaction, which was conducive to the capture and killing of bacteria. The results of the *in vitro* antibacterial experiment demonstrated that the Cip-Ti_3C_2 nanocomposites achieved impressive bactericidal efficiency in inhibiting MRSA. Notably, the most significant bactericidal effect for MRSA was achieved in the Cip-Ti_3C_2 + NIR group. Subsequently, to study the antibacterial mechanism, SEM was used to observe the morphological changes of bacteria of Cip-Ti_3C_2 under NIR laser. Since Cip acts on targets in the bacteria rather than on the bacterial outer membrane, the surface of the Cip-treated cells was as smooth as control, which has no significant change. In contrast, the Cip-Ti_3C_2 group, Ti_3C_2 + NIR group and Cip-Ti_3C_2 + NIR group showed significant deformation of cell morphology and leakage of cell contents. In the MRSA-induced mouse abscess model, hybrid hydrogel had not only lasting antibacterial ability, but also impressive antibacterial efficiency and avoided bacterial rebound after photothermal treatment and thus maximizing the *in vivo* therapeutic effect of the Ti_3C_2 MXene system, which will facilitate further biological applications and clinical translation.

Ag nanoparticles are considered to disturb essential bacterial cell functions through two dominating mechanisms.[73] In the first mechanism, Ag^+ released from the Ag nanoparticles interacts with proteins and enzymes, resulting in serious structural deformation of the bacterial cell membrane. The second

mechanism involves the production of high concentrations of ROS, which perturbs cell metabolism.[74,75] Although Ag nanoparticles enjoy superior antibacterial properties, their high cost and toxicity to the human body (such as argyria, spasms, and gastrointestinal disorders) hamper their wide *in vivo* applications.[76,77] The strategies that minimize Ag^+ concentration while maintaining high antibacterial efficiency are imperative. Currently, Liu *et al.* developed a chemo-photothermal therapy platform (Ag^+-GCS-PDA@GNRs) based on PDA coated gold nanorods (GNRs).[78] The PDA coating had high Ag^+ load efficiency, and a water-soluble chitosan derivative (GCS) with a pH-variant charge ($pK_a \sim 6.5$) could improve biocompatibility and realize acidity-triggered Ag^+ release. In addition, the free amines on the GCS were used to interact with imaging agents (Cy5SE). In the infected area, the environment was acidic, so the nanoplatform showed electropositivity, which could make the nanoplatform more easily have an influence on the infected tissues. Change of pH in infection sites could accelerate the release of Ag^+, and Ag^+ was delivered to the infective area where pH $\sim$ 6.3. In addition, Ag^+ could penetrate the bacterial membrane even at a very low dosage and better the permeability of membrane, and then damage membrane by heat, thus greatly improving the sterilization efficiency of PTT. Simultaneously, increasing temperature could also lead to more Ag^+ release, thus improve the chemotherapy effect of the nanoplatform in turn. Ag^+-GCS-PDA@GNRS combined chemotherapy with thermotherapy completely removed abscesses and promoted wound healing through synergistic antibacterial effects. Taken together, the constructed antibacterial nanoplatforms that facilitate the combination of antibiotics and PTAs offer a promising strategy to address the clinical problems caused by the overuse or misuse of antibiotics.

2.3 Synergistic nitric oxide–photothermal antibacterial therapy

As an endogenous molecule, NO plays an important role in physiological and pathological processes such as wound healing and immune response, and has attracted great attention. Recently, NO has been recognized as a broad-spectrum antibacterial agent. NO can effectively kill bacteria in many ways, either by inducing lipid peroxidation to cause bacterial membrane damage or by forming a large amount of RNS to perturb bacterial metabolisms or by triggering severe oxidative stress that leads to DNA cleavage.[79] In addition, NO can act as a sensitizer to further enhance the antibacterial effectiveness of antibiotics, and to some extent, it can even reverse the drug resistance of cells. Unlike traditional antibacterial agents, NO also promotes wound healing by promoting the debonding and proliferation of epidermal stem cells and increasing the production of muscle fibroblasts and collagen during skin reconstruction. Importantly, the therapeutic efficacy of NO is highly concentration-dependent at the site where it is delivered. NO at high concentrations could cause severe nitrosative and oxidative stresses on cells or bacteria, thus inducing cell apoptosis or bacterial death. NO at low concentrations promotes cell growth and vasodilation. Therefore, to obtain the desired therapeutic effects and minimize the adverse side effects, NO delivery platforms, which can deliver optimal NO dosage in a spatiotemporally-controlled manner to the right site, should be developed. However, because of the short half-life of NO and the lack of suitable NO storage, considerable efforts have been exerted to explore the various NO donors and NO delivery platforms. Among such platforms, light-controlled and heat-controlled NO delivery systems have attracted vast interest due to the ready NO release handed by light.

Based on the above considerations, a multifunctional platform with single NIR laser to trigger PTT and NO release for the collaborative treatment of multidrug resistant bacteria and their biofilms was proposed. *S*-Nitrosothiols (SNOs) are widely distributed in the body. It is the product of sulfhydryl nitrosylation of proteins, polypeptides or thiols, and participates in the storage and transport of NO. Recently, photothermal-sensitive SNO was introduced onto thiolated graphene (TG), and then 4-mercaptophenyl boronic acid, which is a molecular alternative for Gram-negative bacteria detection, was introduced on the surface of TG-NO to obtain TG-NO-B (Fig. 7(a)).[80] Boric acid (BA) is a boron center that connects three hydroxyl groups through carbon–boron bonds, which can covalently bind to diol-containing sugars to form borate esters. Because the surface of Gram-negative bacterial cells contains a lot of lipopolysaccharides containing *cis*-diol groups, BA and its derivatives have been successfully used as recognized molecular substitutes for bacterial detection.[81] In TG-NO-B without laser irradiation, NO was released in a slow and stable manner, with only about 18.8% of NO released within 20 min. In contrast, when treated with continuous laser irradiation (808 nm, 0.75 W cm^{-2}), TG-NO-B showed outbreaking NO release within 5 min, almost 87.7% of NO release. This is because heat generated from nanoplatform could break S–NO bonds, and thus accelerate the release of NO. Under intermittent laser irradiation (30 s every 5 min), NO can be released in a controlled way. When the laser was irradiated at 30 s, the generation of NO increased sharply. After turning off the laser irradiation, the release of NO was greatly reduced. The above results proved that the controllable release of NO can be realized through NIR on/off, and the nanoplatform had potential biomedical application prospects. In addition, TG-NO-B showed good biocompatibility and targeting *in vivo* and *in vitro*. When located at the infected site of Gram-negative bacteria, TG-NO-B could selectively bind to Gram-negative bacterial cells and their biofilm matrix through covalent coupling between boric acid groups and bacterial lipopolysaccharide units, thus greatly improving antibacterial efficiency and reducing adverse side effects on surrounding healthy tissues. Under 808 nm laser irradiation, the bacterial cell membrane was destroyed by the produced high temperature and NO release at the same time, further causing the leakage of intracellular components like DNAs/RNAs, and eventually leading to bacterial death. More importantly, the presence of NO greatly increased the sensitivity of bacterial cells to heat and realized the eradication of bacteria under low-temperature conditions. Diazeniumdiolates (NONOates) are attractive NO donors as they have a wide range of half-life

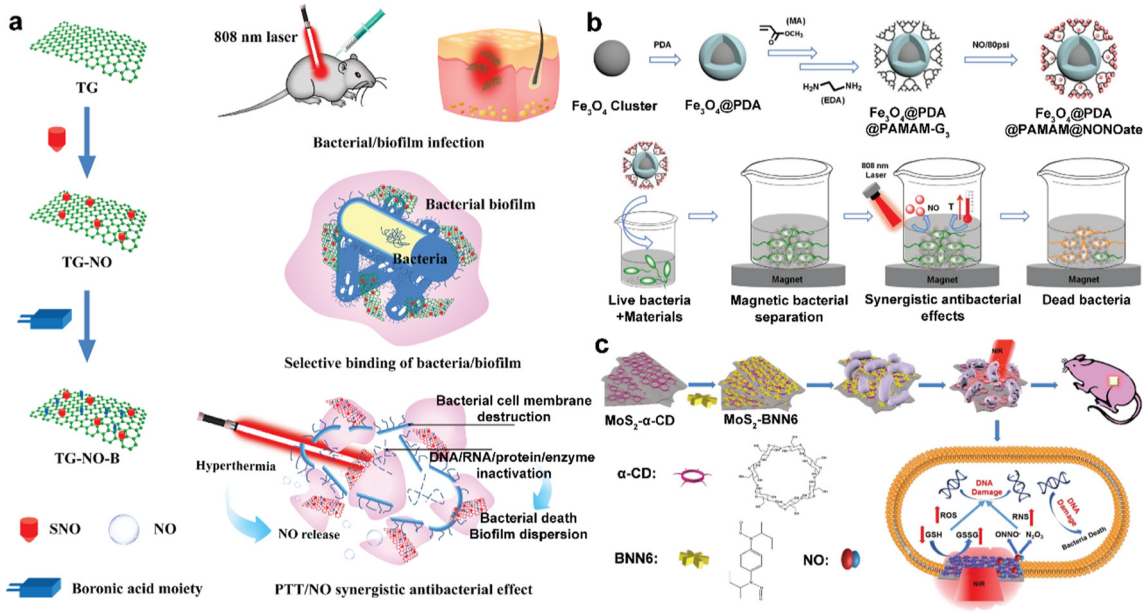

Fig. 7 (a) Schematic illustration of synthetic route and the antimicrobial mechanism of TG-NO-B. Reprinted with permission of ref. 80. Copyright 2020 Springer Nature. (b) Synthetic route and synergistic photothermal and NO killing of bacteria of Fe_3O_4@PDA@PAMAM@NONOate. Reprinted with permission of ref. 83. Copyright 2018 Wiley. (c) Schematic illustration of MoS_2-BNN6 as an NIR laser-mediated NO release nanovehicle for synergistically eliminating bacteria. Reprinted with permission of ref. 84. Copyright 2018 Wiley.

periods from 2 s to 20 h and release 2 moles of NO under physiological conditions.[82] NONOates are usually synthesized by the reaction of primary or secondary amines with NO under high pressure. Dendrimers have attracted considerable interest as effective scaffolds for NO release in combination with NO donors due to their highly branched structure and ample secondary amine moieties. Yu *et al.* used PDA-coated iron oxide nanocomposites (Fe_3O_4@PDA) as photoconverters, grafting first three generations of dendritic poly(amidoamine) (PAMAM-G3) on the surface of Fe_3O_4@PDA and then loading NO on its surface to generate NONOate (Fig. 7(b)).[83] The resultant Fe_3O_4@PDA@PAMAM@NONOate displayed controllable NO release under intermittent 808 nm laser irradiation and excellent bacteria-separation efficiency. As a carrier, the Fe_3O_4@PDA@PAMAM-G3 dispersion showed a concentration-dependent photothermal effect and high photothermal stability. The quantity of the NO payload on Fe_3O_4@PDA@PAMAM-G3 was almost 0.8 μmol mg^{-1} and was almost three times higher than that on pure PDA nanospheres with NO content, indicating that the PAMAM dendrimer could significantly improve the NO loading efficiency of the nanocarriers. Under continuous 808 nm laser irradiation, a sudden release (almost 80%) of NO occurring within the first 1 h was observed. This suggested that laser irradiation could accelerate the release of NO from Fe_3O_4@PDA@PAMAM@NONOates, mainly due to the rapid increase in temperature in the system. When the laser was switched off, NO was released at a much slower rate. In the absence of NO loading, Fe_3O_4@PDA@PAMAM-G3 resulted in a 25% and 15% decrease in the viability of *E. coli* and *S. aureus*, respectively, probably due to its cationic nature. The laser treatment greatly increased the antibacterial capacity of Fe_3O_4@PDA@PAMAM-G3, which must be attributed to the photothermal effect of Fe_3O_4@PDA@PAMAM-G3 by rapidly increasing the temperature of the system, resulting in a 62% and 80% decrease in the viability of *E. coli* and *S. aureus*, respectively. However, the antibacterial activity of Fe_3O_4@PDA@PAMAM@NONOates was further enhanced by NO loading. Interestingly, the difference in the NO-releasing activity of Fe_3O_4@PDA@PAMAM@NONOates against *E. coli* and *S. aureus* may be due to the different membrane properties of these two bacteria. Gram-negative *bacilli* have an additional outer membrane barrier compared to Gram-positive *S. aureus*, which makes them less susceptible to NO release. Studies have shown that the membrane damage in bacteria leads to leakage of intracellular components such as DNA and RNA from the cytoplasm into the surrounding environment, which severely affects bacterial function and eventually leads to bacterial death. Due to the characteristic absorption of DNA and RNA at 260 nm, the optical density at 260 nm (OD_{260}) values can be used to evaluate the situation of DNA and RNA. The groups with Fe_3O_4@PDA@PAMAM@NONOates and laser treatment displayed the highest OD_{260} value, suggesting its strongest destruction of the bacterial membrane, which led to the release of more intracellular components, such as DNA and RNA. For practical applications, it is ideal that the nanomaterials, in particularly those hard to degrade can be removed from the biological environment to reduce their potential health and ecosystem risks. With the aid of the excellent magnetic properties of Fe_3O_4@PDA@PAMAM@NONOates, almost all of the bacteria could be removed by the external magnet in 15 min, as the supernatant turned from the initial turbid suspensions to clear solutions. This study provides a research direction for the construction of an efficient and separable

antibacterial platform. Like 2D graphene, nano-sized MoS_2 nanosheets can also be used as a delivery system for NO donors, owing to its advantages such as large surface area, easy surface modification, and high NIR-responsive photothermal conversion properties. The BNN6 is a UV-vis light-responsive NO donor that does not respond to NIR light. However, the release of NO from BNN6 can be triggered by the heat generated during the PTT process. So BNN6 is usually loaded into NIR-responsive PTAs *via* π–π stacking interaction. Gao *et al.* presented a new 808 nm laser NO release nanocarrier (MoS_2-BNN6), which was developed by the simple assembly of α-cyclodextrin-modified MoS_2 nanosheets with the thermosensitive NO donor BNN6. This nanoplatform can achieve highly effective and timely antibacterial treatment against three typical bacteria, including Gram-negative and Gram-positive bacteria (ampicillin-resistant *E. coli*, heat-resistant *Escherichia faecalis* (*E. faecalis*)), and a pathogen (*S. aureus*) (Fig. 7(c)).[84] When trapped by bacteria, MoS_2-BNN6 makes NO diffuse to the surface of bacteria more easily, and when exposed to 808 nm laser irradiation, the release of NO became controllable and precise. At the same time, the high temperature induced by MoS_2 under 808 nm radiation accelerated the oxidation of the antioxidant glutathione to disulfide, thereby disrupting the balance of antioxidants in bacteria. More importantly, the synergistic treatment effectively killed heat-resistant *E. faecalis* (98%), which was attributed to the following points: (1) MoS_2-BNN6 + NIR could realize synergistic PTT/NO antibacterial activity in one nanocarrier, and achieve enhanced oxidative/nitrosative stress and even DNA damage; (2) MoS_2-BNN6 + NIR could accelerate the oxidation of glutathione, thus reducing the usage of ROS/RNS generated in bacteria, and thus improve the antibacterial efficiency. This work will provide an experimental basis for the complete eradication of some usual bacteria which are resistant to normal drug and high temperature.

Recently, Janus nanoparticles (JNPs) have received considerable attention in drug delivery, due to their unique anisotropic surface properties, heterostructure, surface properties, and integrated functionalities. Among them, metal-based JNPs, such as metal–polymer, metal–metal, and metal–oxide JNPs, have become an active frontier of research due to the combination of chemical properties, surface plasmon resonance (SPR), electronic features derived from metal, and diversified properties from other materials. Liang *et al.* designed and synthesized a type of gold nanostar/hollow dopamine Janus nanostructure (GNS/HPDA-BNN6) with photothermal activity and accurate NIR light-controlled NO release performance.[85] First, small Au nanoparticles were decorated on the surface of hollow PDA. Subsequently, using a modified seed-mediated synthetic method, Au^+ ions were grown along Au nanoparticles to form gold nanostar/hollow dopamine Janus nanostructure (GNS/HPDA JNPs). Finally, BNN6, which is a typical *N*-nitrosamine NO donor, was loaded into GNS/HPDA JNPs through a special π–π stacking interaction (Fig. 8(a)). To explore the antibacterial effect of NO release GNS/HPDA-BNN6, Gram-negative *bacillus* and Gram-positive *S. aureus* were modelled. BNN6 itself had no inhibitory effect on bacteria. It is worth noting that GNS/HPDA-BNN6 irradiated by NIR lasers had a strong antibacterial effect. When the drug concentration was 200 μg mL^{-1}, it completely inhibited the growth of the two bacteria on the plate. PTT (GNS/HPDA + NIR) could consume 54% glutathione (GSH) in MRSA, and this percent will be up to 80% when it was combined with NO release. As more and more drug-resistant bacteria have appeared, the ability to eradicate biofilms is necessary to an antibacterial nanoplatform. As shown in Fig. 8(b), after 48 h of incubation, a thick and dense bacterial biofilm could be clearly seen in the control group, indicating that a proper MRSA biofilm model was well established. GNS/HPDA and GNS/HPDA-BNN6 treatments almost had no biofilm eradication ability. Individual photothermal effect (GNS/HPDA + NIR) could damage part of biofilms, and synergistic PTT and NO (GNS/HPDA-BNN6 + NIR) can achieve best efficiency on eradicating biofilms, even the concentration of GNS/HPDA-BNN6 + NIR treatment was less than 200 μg mL^{-1}. Genome analysis of the MRSA strain was conducted to find out the mechanism of PTT and NO antibacterial therapy before and after GNS/HPDA-BNN6 + NIR. Under photothermal and NO therapy, the significant upregulations of many genes responsible for metabolism regulation in the MRSA strain revealed the increased production of intracellular ROS and $^{\bullet}OH$ (Fig. 8(c), left); the downregulations of the membrane-associated genes indicated that the functions of the bacterial membrane were largely disturbed (Fig. 8(c), right). Moreover, PTT combined with NO could diminish drug-resistant MRSA through downregulating the expression of relative genes. Therefore, the main mechanism of the synergistic photothermal and NO antibacterial effect involved that the synergistic PTT and NO could destruct cell membrane and lead to leakage of intracellular components and the nanoplatform also interfered with the metabolism of the bacteria by up or downregulating genes (Fig. 8(d)). We believe that using a bacterial gene analysis method to obtain an in-depth antibacterial mechanism will provide technical support for the construction of an excellent synergistic antibacterial platform. Due to their high absorbance coefficient and excellent stability under physiological conditions, the development of NIR J-aggregates has received increasing attention in biomedical fields.[86,87] Typical organic dyes are usually candidate molecules for constructing J-aggregates. Recently, several aza-boron dipyrromethene (aza-BODIPY) derivatives have been developed and their biomedical applications have been evaluated.[88,89] Notably, the structural engineering of aza-BODIPY dyes can efficiently inhibit intermolecular aromatic interactions, thereby accelerating the formation of J-aggregates. Interestingly, the use of NO-releasing moieties can regulate the aggregation behavior of organic dyes. Bao *et al.* designed a new NIR J-aggregate with NO-releasing aza-BODIPY (BDP-NO) *via* the nitrosation of an amine-containing aza-BODIPY precursor (BDP-NH_2). Subsequently, BDP-NO was loaded into poly(ethylene glycol)-*b*-poly(ε-caprolactone) (PEG-*b*-PCL) micellar nanoparticles, and then accelerated the formation of J-aggregates of BDP-NO. The resulting nanoparticles showed controllable antibacterial effect including either NO release, PTT, or a combination of NO and PTT (Fig. 9(a)).[90]

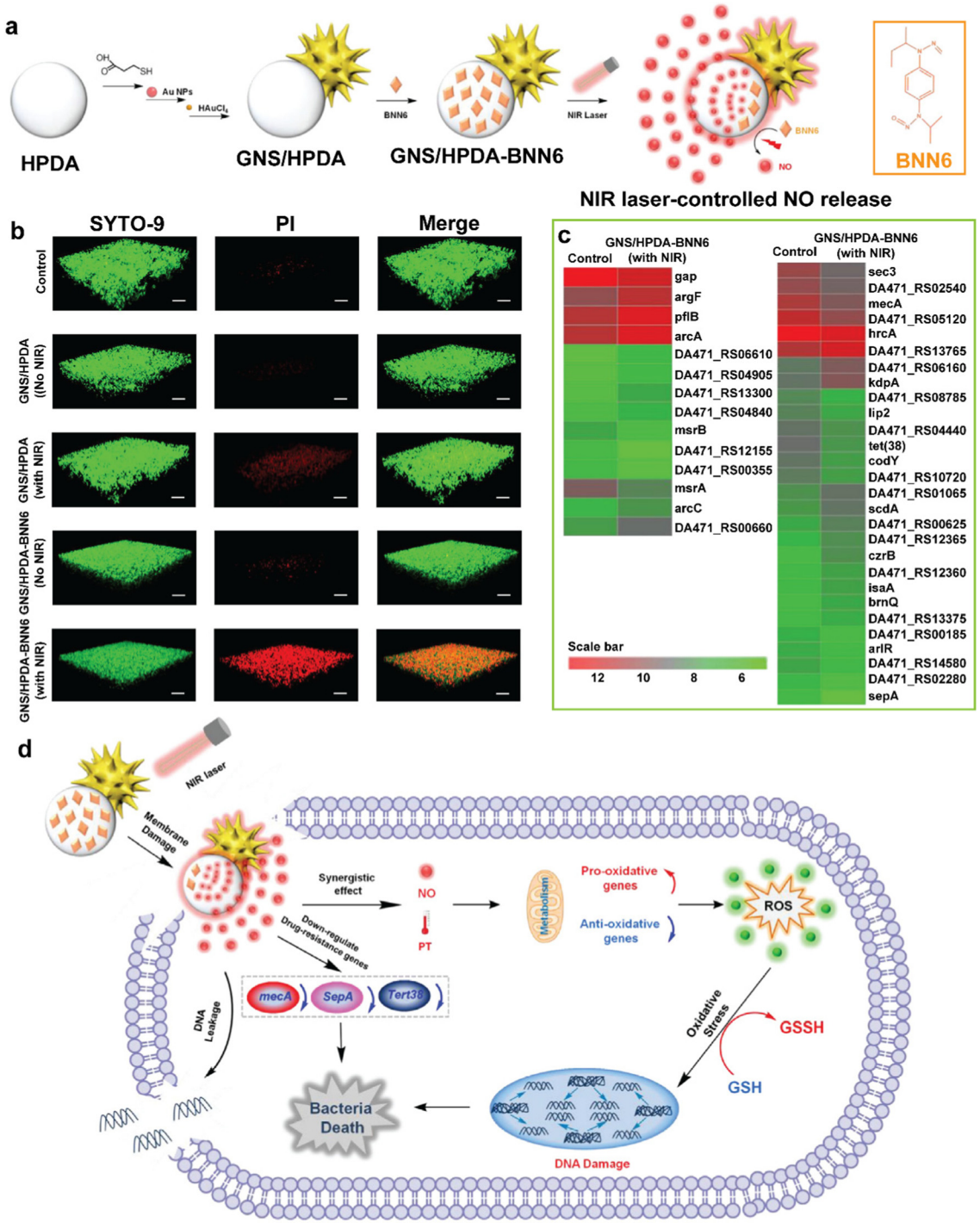

Fig. 8 (a) Synthetic route of GNS/HPDA, GNS/HPDA-BNN6, and the NIR laser-controlled NO release properties of GNS/HPDA-BNN6. (b) Evaluation of the synergistic photothermal and NO anti-biofilm activity of GNS/HPDA-BNN6 against MRSA. Confocal images show the biofilm eradication efficiency of different treatments, where dead bacteria stained by PI dye emit red fluorescence. The scale bar represents 30 μm. (c) Genome analysis to determine the mechanism of the synergistic photothermal and NO antibacterial effect of GNS/HPDA-BNN6 against MRSA. Heat map showing the expression level of differentially expressed genes related to bacterial metabolism (left) and to membrane integrity, substrate transport, transcription and translation, and drug resistance (right) in the GNS/HPDA-BNN6 + NIR-treated and control groups. The number in the scale bar represents the logarithmic value of the expression levels. Green indicates low expression levels, and red indicates the high expression level. (d) The proposed antibacterial mechanism of the synergistic photothermal and NO antibacterial effect of GNS/HPDA-BNN6 under NIR laser irradiation. Reprinted with permission of ref. 85. Copyright 2022 Elsevier.

The feeding ratios of PEG-*b*-PCL and BDP-NO could adjust the loading efficiency of BDP-NO. Specifically, as the loading efficiency improved, the maximal absorbance peaks gradually red-shifted from ≈711 nm of NP-1 (the feeding ratio was 1 wt%)

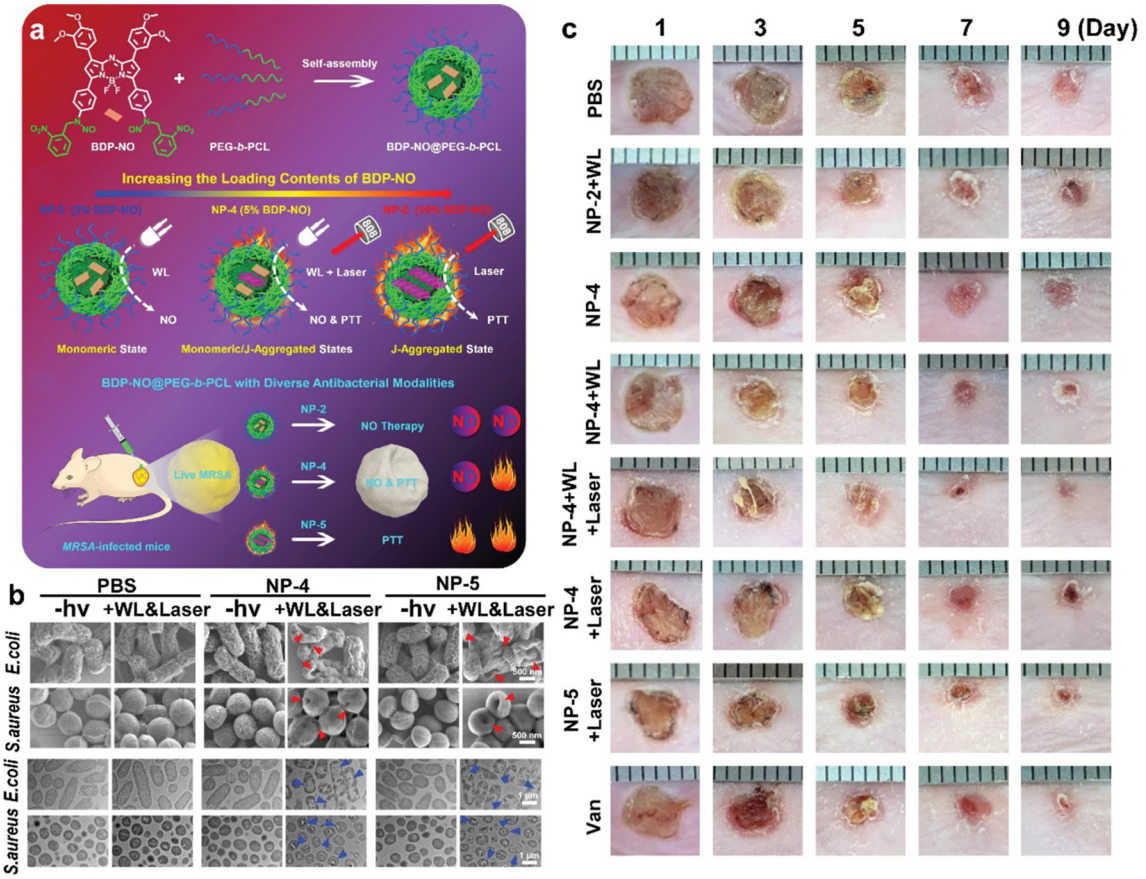

Fig. 9 (a) Schematic illustration of the formation, the aggregation states and treatment of MRSA infection by BDP-NO@PEG-*b*-PCL micellar nanoparticles (WL = white light, PTT = photothermal therapy). (b) SEM images and TEM images of *E. coli* (top panel) and *S. aureus* (bottom panel) in the absence and presence of NP-4 or NP-5 micelles (0.333 g L^{-1}) without or with irradiation. The red triangles highlight the collapsed bacteria with disrupted bacterial membranes, while the blue triangles indicate the loss of intracellular contents after treatments. (c) Photographs of cutaneous wounds of MRSA-infected mice receiving various treatments. Reprinted with permission of ref. 90. Copyright 2022 Wiley.

to ≈820 nm of NP-5 (the feeding ratio was 10 wt%) micelles, indicating the formation of J-aggregates within micellar nanoparticles. Impressively, the excellent PCE may be attributed to the inhibited fluorescence emission of BDP-NO in the presence of NO-releasing moieties.[91] As such, the integration of NO-releasing moieties not only provided a new means to alter the aggregation behavior of organic dyes but also improved PCE by inhibiting radiative decay. At a low loading ratio of BDP-NO, NP-2 (the feeding ratio was 2 wt%) micelles released NO under white light irradiation; at a medium loading ratio, NP-4 (the feeding ratio was 5 wt%) micelles released NO and had a PTT effect with NIR; at the highest loading ratio, NP-5 micelles served as a PTT agent without evident NO release (Fig. 9(a)). The *in vitro* antibacterial experiment results proved that at a micelle concentration of 0.333 mg mL^{-1}, NP-4 micelles could kill almost all drug-resistant bacteria under sequential white light and NIR, which was much more efficient than NP-2 at the same concentration. At a micelle concentration of 0.617 mg mL^{-1}, NP-5 micelles had enhanced PCE under NIR compared to that of NP-4 micelles. The results of SEM and TEM showed that only NP-4 or NP-5 under NIR could lead to evident morphological changes and holes in bacterial membranes. Moreover, the loss of cytoplasmic contents could be readily observed by TEM (Fig. 9(b)). Next, the *in vivo* antibacterial applications of BDP-NO@PEG-*b*-PCL micelles in MRSA-infected skin wound model were evaluated (Fig. 9(c)). NP-2 micelles under white light showed a little more sufficient therapy compared to the PBS control; this is because of the photo-mediated NO release.

NP-4 micelles with sequential white light and NIR laser irradiation showed faster wound healing than vancomycin and the other groups. Although NP-5 micelles with NIR laser irradiation showed the best bacterial killing effect in *in vitro* antibacterial experiments, its side effect like hyperthermia can induce inflammation and inhibit wound healing. Notably, NP-4 micelles with white light irradiation and NIR laser irradiation displayed the most satisfactory antibacterial effect, likely due to NO in accelerating wound healing. This work opened a new way to integrate NO-releasing molecules and NIR J-aggregates for potential biomedical applications.

Synergistic NO–photothermal antibacterial therapy, as a new treatment method, has attracted much attention in recent years. On the one hand, PTT can effectively destroy the bacterial cell wall and promote NO penetration into the bacterial cell. On the other hand, nanoplatforms with NIR-responsive NO generation and PTT can disperse and eradicate mature

biofilms. Importantly, the release of NO can modulate the inflammatory immuno-response to reduce tissue damage. Therefore, we think that synergistic NO/PTT will be a very promising antibacterial method in the future.

2.4 Synergistic new treatment-photothermal antibacterial therapy

Sonodynamic therapy (SDT) combines acoustic sensitizers and low-intensity ultrasound to open up new ways to treat drug-resistant bacteria. It can concentrate the energy of ultrasound in the bacterial infection site buried deep in the tissue, locally activate the sensitizer, and produce cytotoxic ROS that can induce bacterial death.[92] Possible mechanisms of SDT include the mechanical stress of ultrasound and the cytotoxicity effect of ROS. Mechanical effects mainly include cavitation effect and sonoporation effect. Cavitation effect refers to a unique phenomenon caused by the interaction between ultrasound and the water environment. This process includes nucleation, growth and implosion of bubbles. In essence, cavitation can be divided into stable cavitation and inertial cavitation. Acoustic emission, microflow, jet and shock wave generated by inertial cavitation will cause mechanical damage to bacteria. The sonoporation effect refers to the formation of holes on the surface of the cell membrane under ultrasonic irradiation. The shear stress and microfluence caused by cavitation will produce temporary stoma on the cell membrane. The sonoporation effect can improve the permeability of drugs to cell membranes and allow molecules or nanoparticles to pass through the cell membrane, thus increasing the accumulation of drugs in cells. In addition to the mechanical effect of ultrasound, cytotoxic ROS produced by acoustic sensitizer is considered to be an effective way to the sterilization of SDT. Sonoluminescence is the most common ROS formation mechanism in SDT, which refers to the very short-term light emission excited by the energy released by the rapid implosion of bubbles during cavitation.[93] Sonoluminescence is mainly related to inertial cavitation, because the energy released by bubble rupture during inertial cavitation can stimulate the production of photons. At the same time, another mechanism produced by SDT inducing ROS is called ''pyrolysis''. During inertial cavitation, the energy released by bubble implosion causes the surrounding microenvironment to reach a temperature of up to 10 000 K and a pressure of up to 81 MPa. Due to high temperature and high pressure, the acoustic agent is pyrolyzed and then interacts with O_2 to form ROS. So far, several metal peroxide nanoparticles have been developed for antibacterial use, but at this stage, their reactivity is difficult to regulate, and the oxidation reaction is easy to be triggered, thus causing toxic and side effects on healthy tissues. Therefore, it is advisable to combine SDT with PTT to overcome its disadvantage, at the same time decrease the thermal damage to normal tissue by PTT. Bi *et al.* synthesized a new nanomaterial, silver peroxide nanoparticles (Ag_2O_2 NPs), as a potential antibacterial drug.[94] Ag_2O_2 NPs were reasonably designed as a new generation of stimulating response metal oxide nanoparticles as a reactant of hydrogen peroxide (H_2O_2) and oxygen to induce oxidative stress. Subsequently, the transition metal catalyzed H_2O_2 to produce $^{\bullet}OH$ through Fenton-like reactions. The $^{\bullet}OH$ was the main ROS species induced by ultrasound radiation, followed by $^1O_2$, and O^{2-} played a secondary role. Ag_2O_2 nanoparticles showed attractive photothermal conversion ability and good photothermal stability under NIR light, with a PCE (η) of 41.5%. Therefore, most photosensitive agents have the potential to act as acoustic sensitizers. Acoustic sensitizers could be activated from the ground state to the excited state at a specific ultrasound frequency. When returning to the ground state, the acoustic sensitizer could transfer the released energy to oxygen to produce ROS. Compared with NIR (tissue penetration depth $\leq$2 cm), the depth of ultrasound in soft tissue could even reach more than 10 cm, making up for the shortcomings of PTT in tissue penetration ability.

Sometimes the curative effect of PTT is compromised by the collateral damage to healthy tissues due to the lack of bacterial targeting. In order to improve specificity of treatment, PTT combined immunotherapy has attracted people's attention in the antibacterial field. Advanced immunoconjugate means modifying adjuvants or targeted antigens to antibacterial agents to mediate complex immune responses through specific identification, immune blocking and immune cell collection. They are not only toxic to bacterial cells, but also retain the ability to recognize specific bacterial antigens.[95] Zhao *et al.* developed nano neuro-immune blockers (NNIBs) by modifying an immune escape membrane exterior on the surface of the Au nanocages (Au NCs).[96] Based on the competitive membrane functions of the glioma cell membrane, NNIBs could target the toxins produced by *S. pyogenes* so as to neutralize streptolysin S (SLS), which would otherwise inhibit the generation of neutrophils. Herein, NNIBs performed well in inhibiting pain conduction and enhancing the host immune defense for invasive bacterial infection. Synchronously, the high temperature generated by PTT of Au NC can effectively create an acute inflammatory environment for recruiting more immune cells and enhancing hosts' immune defense against bacterial infections. Li *et al.* prepared a photoexcited hydroxyapatite (Hap)/nitrogen-doped carbon dot (NCDS) modified graphene oxide (GO) heterojunction film (GO/NCD/Hap), which promoted the separation of interface electrons and holes and inhibited the compound efficiency through hole depletion, so it had enhanced photocatalysis and photothermal effects.[97] At the same time, the electron transfer between the film and the cell membrane after irradiation induced the flow of calcium ions in cells, promoted the migration and proliferation of cells, and facilitated the enhancement of alkaline phosphatase, thus realized tissue reconstruction. *In vivo* experiment showed that the repair of vascular injury was achieved through a Ca-activated PLCγ1/ERK pathway, which was characterized by enhanced CD31 expression. In addition, the increased $CD4^+$/$CD8^+$ lymphocytes had also been improved by activating the PI3K/P-AKT pathway. Therefore, electron metastasis enhances the effect of collaborative PDT and PTT treatment of bacterial infections through immune therapy.[98] We believe that the combination of PTT and SDT or immunotherapy will be

anticipated to have more application prospects due to the minimal invasive nature and higher antibacterial effect in the future.

3. Conclusions and perspectives

In recent years, the growing problem of antibiotic resistance has made the traditional antibiotic therapy of many infectious diseases less efficient. Antibiotic-resistant bacteria display resistance by antibiotic inactivation, exclusion from the internal environment, target alteration, production of an alternative target, and so on. Fortunately, various antibacterial approaches, which do not rely on traditional therapeutic regimens, have been developed. One of the most interesting is NIR light-mediated PTAT owing to its target selectivity, remote controllability, minimal non-invasiveness, fast and effective treatment, and favorable biosafety in normal tissues. In PTAT, once photothermal materials are excited by the absorption of light with a suitable wavelength, photons can interact with the lattice to cause the lattice to vibrate. A rapid increase in temperature will destroy bacterial membranes and proteins and finally inactivate the bacteria. However, the use of PTAT alone to completely eradicate bacteria usually requires a local temperature increase to more than 70 °C or long-term high temperature, which may cause an inflammatory response and thermal damage to nearby healthy tissues. Combined therapy based on two or more treatments can overcome the defects of monotherapy and achieve reduced toxicity and enhanced efficiency. In this review, we systematically summarized the research progress of multimodal bactericidal nanoplatform based synergistic PTAT, including photodynamic–photothermal, chemo-photothermal and NO–photothermal antibacterial therapies. We also discussed how synergistic PTAT can work on bacteria to inhibit infection. Despite recent achievements in photothermal-based synergistic therapy in the antibacterial field, many challenges and critical issues remain to be addressed in the future. Therefore, for the development of more effective and safer antibacterial therapy, future research should also consider the following aspects:

(1) The targeting of antibacterial agents

Considering the influence of photothermal nanoplatforms on normal tissues around infected sites during treatment, improving the targeting of nanoplatforms for bacteria is also a promising way of reducing toxicity and enhancing efficiency. However, the precise positioning of synergistic PTAs in bacteria has not yet been fully explored. Recent developments have greatly enriched our knowledge that the material surface plays a decisive role in antibacterial processes. Therefore, it is necessary to develop advanced surface modification strategies to enhance the bactericidal effect at the location of the lesion, thereby reducing the interaction between the material and the normal tissue. In general, bacterial cells are coated with a peptidoglycan layer (consisting of sugars and amino acids), which means that most bacteria are negatively charged. Thus, positively charged material surfaces are widely used to capture bacteria through electrostatic interactions. Cationic molecules (*e.g.*, quaternary ammonium salt) can kill bacteria effectively based on the contact-killing effect. However, cationic molecules are often associated with high charge-related toxicity. Therefore, non-toxic cationic chitosan derivatives have been introduced on the surface of nanomaterials to reduce cytotoxicity and enhance targeting.[99,100] In addition to the electrostatic attraction mentioned above, receptor–ligand interactions are also an effective strategy to target characteristic molecules in the bacterial cell wall. Using a carbohydrate-binding protein on the surface of bacteria, glycan derivatives have been widely used in antibacterial material modification to target bacteria.[101] Furthermore, homologous targeting of antibacterial agents using the surface coating of the bacterial cell membrane will be an important research direction to achieve high targeting in the future.

(2) The permeability of antibacterial agents

Gene mutation and phenotypic changes within the biofilms and the protection of the extracellular matrix play an important role in resisting drug penetration and the development of bacterial resistance. For the tricky problem of biofilms, the main dilemma in bacterial sterilization and biofilm elimination is the low penetration and diffusion of antibacterial agents through the extracellular matrix into the internal biofilms.[102] As a result, the main strategy to increase the penetration amounts of antibacterial agents into biofilms is increasing the concentration of antimicrobial agents. However, high concentrations of antibacterial agents result in cytotoxicity, immunophagocytosis, and potential metabolic problems. Considering the high adhesion and penetration of the sharp structure to the surface, it is expected to increase the penetrating ability of antibacterial agents into cell membranes. For example, needle-like antibacterial agents can pierce into bacterial walls or biofilms and efficiently deliver PTAs or antibiotics to infected sites without the development of bacterial resistance.

(3) Customization of synergistic photothermal antibacterial therapy

According to the characteristics of the infected site, customization of more specialized synergistic photothermal antibacterial methods will provide a new idea for low toxicity and high-efficiency antibacterial treatment. For example, impaired wounds in diabetic patients are difficult to heal, which seriously threatens public health. The delayed transition from the inflammatory stage to the proliferation stage limits the recovery of diabetic wounds. In addition, bacterial infections in diabetic wounds can aggravate inflammatory conditions and hinder wound closure. Therefore, diabetic wounds are a chronic clinical complication. Some studies have shown that macrophages play a key role in regulating the inflammation-proliferative phase transition in traumatized environments.[103] During the inflammatory stage, the M1 phenotype of the wound can remove damaged tissue. Under healthy conditions, macrophages differentiate into an anti-inflammatory and regenerative M2 phenotype, which enters the proliferation stage by

preventing excessive inflammation and promoting stromal cell proliferation and angiogenesis. Unfortunately, under pathological conditions, such as diabetes or bacterial infection, macrophages cannot be converted from the M1 phenotype into the M2 phenotype. Therefore, according to the characteristics of diabetes, customization of PTAT combined with an adjustable phenotype of macrophages for antibacterial activity will contribute to the recovery of diabetes. Fortunately, curcumin is a natural polyphenol extracted from turmeric and is recognized as an anti-inflammatory wound healing agent. Curcumin also has the ability to polarize macrophages from the M1 phenotype to the M2 phenotype, making it a potential therapeutic agent for diabetic wounds. Therefore, synergistic M2-macrophage polarization and PTAT will provide a new research idea for the complete cure of bacteria-infected diabetic wounds.

(4) The development of an evaluation method for antimicrobial efficacy

With the increase in the type of treatments, more advanced and intuitive evaluation methods have become necessary. For example, the extracellular polysaccharides in the biofilm can be stained with crystalline violet dye. Then, the content of the extracellular polysaccharides can be measured, and the state of the biofilm can be confirmed. In addition, because synergistic photothermal effects can induce differentially expressed genes and significantly enrich metabolic pathways, genes with functions in transcription and translation are also affected. Therefore, the study of antibacterial effects at the gene level will be a new way to understand the antibacterial mechanism in the future.

In summary, the development of multifunctional PTT-based antibacterial materials has provided an opportunity for attenuated and efficient antibacterial therapy. More efforts are still needed for comprehensive investigation of the biosafety and potential side effects of these antimicrobial materials before their practical application in biomedical devices. We believe that strong cross-disciplinary collaboration can lead to rapid developments in this field, as a result of which synergistic PTT will be widely used in practical antibacterial applications in the near future.

Conflicts of interest

There are no conflicts to declare.

Acknowledgements

This study was financially supported by the National Natural Science Foundation of China (No. 22175122), the Foundation of Liaoning Educational Committee (No. LJKZ0932), the Excellent Young Scholars Program of Shenyang Pharmaceutical University (No. YQ202114), the Career Development Support Plan for Young and Middle-aged Teachers in Shenyang Pharmaceutical University (No. ZQN2021003), and the Shenyang Young and Middle-aged Scientific and Technological Innovation Talents Support Project (No. RC220420).

Notes and references

1 Y. Ding, Z. Yuan, J.-W. Hu, K. Xu, H. Wang, P. Liu and K.-Y. Cai, Surface modification of titanium implants with micro-nano-topography and NIR photothermal property for treating bacterial infection and promoting osseointegration, *Rare Met.*, 2022, **41**, 673–688.
2 B. H. Nataraj and R. H. Mallappa, Antibiotic resistance crisis: an update on antagonistic interactions between probiotics and methicillin-resistant staphylococcus aureus (MRSA), *Curr. Microbiol.*, 2021, **78**, 2194–2211.
3 L. Jiang and S. C. J. Loo, Intelligent nanoparticle-based dressings for bacterial wound infections, *ACS Appl. Bio Mater.*, 2021, **4**, 3849–3862.
4 A. H. T. Kafa, G. Tüzün, E. Güney, R. Aslan, K. Sayin, B. Tüzün and H. Ataseven, Synthesis, computational analyses, antibacterial and antibiofilm properties of nicotinamide derivatives, *Struct. Chem.*, 2022, **3**, 1189–1197.
5 M. H. Ahmed, M. T. Javed, S. U. K. Bahadur, A. Tariq, M. H. Tahir, M. E. Tariq, N. Tariq, S. Zarnab and M. H. Ali, Antibacterial effects of copper oxide nanoparticles against E. coli induced infection in broilers, *Appl. Nanosci.*, 2022, **12**, 2031–2044.
6 P. Cardoso, H. Glossop, T. G. Meikle, A. Aburto-Medina, C. E. Conn, V. Sarojini and C. Valery, Molecular engineering of antimicrobial peptides: microbial targets, peptide motifs and translation opportunities, *Biophys. Rev.*, 2021, **13**, 35–69.
7 A. Choudhury, S. M. A. Islam, M. R. Ghidey and C. M. Kearney, Repurposing a drug targeting peptide for targeting antimicrobial peptides against Staphylococcus, *Biotechnol. Lett.*, 2020, **42**, 287–294.
8 N. Baker, A. J. Williams, A. Tropsha and S. Ekins, Repurposing quaternary ammonium compounds as potential treatments for COVID-19, *Pharm. Res.*, 2020, **37**, 104.
9 C. B. Lineback, C. A. Nkemngong, S. T. Wu, X. B. Li, P. J. Teska and H. F. Oliver, Hydrogen peroxide and sodium hypochlorite disinfectants are more effective against Staphylococcus aureus and Pseudomonas aeruginosa biofilms than quaternary ammonium compounds, *Antimicrob. Resist. Infect. Control*, 2018, **7**, 154.
10 R. Pluta, D. R. Boer, F. L.-Díaz, S. Russi, H. Gómez, C. F.-López, R. P.-Luque, M. Orozco, M. Espinosa and M. Coll, Structural basis of a histidine-DNA nicking/joining mechanism for gene transfer and promiscuous spread of antibiotic resistance, *Proc. Natl. Acad. Sci. U. S. A.*, 2017, **114**, E6526–E6535.
11 C. Piras, A. Soggiu, V. Greco, P. A. Martino, F. D. Chierico, L. Putignani, A. Urbani, J. E. Nally, L. Bonizzi and P. Roncada, Mechanisms of antibiotic resistance to enrofloxacin in uropathogenic Escherichia coli in dog, *J. Proteomics*, 2015, **127**, 365–376.

12 S. B. Neogi, M. M. Islam, S. K. S. Islam, A. H. M. T. Akhter, Md. M. H. Sikder, S. Yamasaki and S. M. L. Kabir, Risk of multi-drug resistant Campylobacter spp. and residual antimicrobials at poultry farms and live bird markets in Bangladesh, *BMC Infect. Dis.*, 2020, **20**, 278.
13 R. Peraman, S. K. Sure, V. N. A. Dusthackeer, N. B. Chilamakuru, P. R. Yiragamreddy, C. Pokuri, V. K. Kutagulla and S. Chinni, Insights on recent approaches in drug discovery strategies and untapped drug targets against drug resistance, *Future J. Pharm. Sci.*, 2021, **7**, 56.
14 Z. H. Bao, K. X. Li, P. P. Hou, R. Xiao, Y. Yuan and Z. H. Sun, Nanoscale metal–organic framework composites for phototherapy and synergistic therapy of cancer, *Mater. Chem. Front.*, 2021, **5**, 1632–1654.
15 H. L. Ou, J. Li, C. Chen, H. Q. Gao, X. Xue and D. Ding, Organic/polymer photothermal nanoagents for photoacoustic imaging and photothermal therapy in vivo, *Sci. China Mater.*, 2019, **62**, 1740–1758.
16 Y.-S. Liu, X. Wei, X. Zhao, L.-J. Chen and X.-P. Yan, Near-infrared photothermal/photodynamic-in-one agents integrated with a guanidinium-based covalent organic framework for intelligent targeted imaging-guided precision chemo/PTT/PDT sterilization, *ACS Appl. Mater. Interfaces*, 2021, **13**, 27895–27903.
17 Y. Ye, J. He, Y. Qiao, Y. C. Qi, H. B. Zhang, H. A. Santos, D. Zhong, W. L. Li, S. Y. Hua, W. Wang, A. Grzybowski, K. Yao and M. Zhou, Mild temperature photothermal assisted anti-bacterial and anti-inflammatory nanosystem for synergistic treatment of post-cataract surgery endophthalmitis, *Theranostics*, 2020, **10**, 8541–8557.
18 W. Qian, C. Yan, D. F. He, X. Z. Yu, L. Yuan, M. L. Liu, G. X. Luo and J. Deng, PH-triggered charge-reversible of glycol chitosan conjugated carboxyl graphene for enhancing photothermal ablation of focal infection, *Acta Biomater.*, 2018, **69**, 256–264.
19 Y. Yang, L. Ma, C. Cheng, Y. Y. Deng, J. B. Huang, X. Fan, C. X. Nie, W. F. Zhao and C. S. Zhao, Nonchemotherapic and robust dual-responsive nanoagents with on-demand bacterial trapping, ablation, and release for efficient wound disinfection, *Adv. Funct. Mater.*, 2018, **28**, 1705708.
20 M. Moun and R. Singh, Metal–semiconductor interface engineering in layered 2D materials for device applications, *Bull. Mater. Sci.*, 2021, **44**, 223.
21 C. Zhang, D.-F. Hu, J.-W. Xu, M.-Q. Ma, H. B. Xing, K. Yao, J. Ji and Z. Xu, Polyphenol-assisted exfoliation of transition metal dichalcogenides into nanosheets as photothermal nanocarriers for enhanced antibiofilm activity, *ACS Nano*, 2018, **12**, 12347–12356.
22 Z. H. Li, X. C. Feng, S. T. Gao, Y. Jin, W. C. Zhao, H. F. Liu, X. J. Yang, S. Q. Hu, K. Cheng and J. C. Zhang, Porous organic polymer-coated band-aids for phototherapy of bacteria-induced wound infection, *ACS Appl. Bio Mater.*, 2019, **2**, 613–618.
23 X. L. Qi, Y. J. Huang, S. Y. You, Y. J. Xiang, E. Cai, R. Mao, W. H. Pan, X. Q. Tong, W. Dong, F. F. Ye and J. L. Shen, Engineering robust Ag-decorated polydopamine nano-photothermal platforms to combat bacterial infection and prompt wound healing, *Adv. Sci.*, 2022, **9**, 2106015.
24 X. J. Zhu, W. Feng, J. Chang, Y.-W. Tan, J. C. Li, M. Chen, Y. Sun and F. Y. Li, Temperature-feedback upconversion nanocomposite for accurate photothermal therapy at facile temperature, *Nat. Commun.*, 2016, **7**, 10437.
25 J. Zhao, S. Y. Huang, P. Ravisankar and H. J. Zhu, Two-dimensional nanomaterials for photoinduced antibacterial applications, *ACS Appl. Bio Mater.*, 2020, **3**, 8188–8210.
26 J.-W. Xu, K. Yao and Z.-K. Xu, Nanomaterials with a photothermal effect for antibacterial activities: an overview, *Nanoscale*, 2019, **11**, 8680–8691.
27 H. C. Han, J. J. Yang, X. Y. Li, Y. Qi, Z. Y. Yang, Z. J. Han, Y. Y. Jiang, M. Stenzel, H. Li, Y. X. Yin, Y. Du, J. R. Liu and F. L. Wang, Shining light on transition metal sulfides: New choices as highly efficient antibacterial agents, *Nano Res.*, 2021, **14**, 2512–2534.
28 J. L. Huang, J. F. Zhou, J. Y. Zhuang, H. Z. Gao, D. H. Huang, L. X. Wang, W. L. Wu, Q. B. Li, D.-P. Yang and M.-Y. Han, Strong near-infrared absorbing and biocompatible CuS nanoparticles for rapid and efficient photothermal ablation of Gram-positive and -negative bacteria, *ACS Appl. Mater. Interfaces*, 2017, **9**, 36606–36614.
29 X. Y. Liu, X. Y. Li, Y. Shan, Y. X. Yin, C. R. Liu, Z. Y. Lin and S. S. Kumar, CuS nanoparticles anchored to g-C_3N_4 nanosheets for photothermal ablation of bacteria, *RSC Adv.*, 2020, **10**, 12183–12191.
30 T. Briggs, G. Blunn, S. Hislop, R. Ramalhete, C. Bagley, D. McKenna and M. Coathup, Antimicrobial photodynamic therapy-a promising treatment for prosthetic joint infections, *Lasers Med. Sci.*, 2018, **33**, 523–532.
31 X. Qin, C. Wu, D. C. Niu, L. M. Qin, X. Wang, Q. G. Wanga and Y. S. Li, Peroxisome inspired hybrid enzyme nanogels for chemodynamic and photodynamic therapy, *Nat. Commun.*, 2021, **12**, 5243.
32 X. F. Teng, X. M. Liu, Z. D. Cui, Y. F. Zheng, D.-F. Chen, Z. Y. Li, Y. Q. Liang, S. L. Zhu and S. L. Wu, Rapid and highly effective bacteria-killing by polydopamine/IR780@MnO_2-Ti using near-infrared light, *Prog. Nat. Sci.: Mater. Int.*, 2020, **30**, 677–685.
33 Y. Q. Zhang, J. Fang, S. Y. Ye, Y. Zhao, A. Wang, Q. L. Mao, C. X. Cui, Y. L. Feng, J. C. Li, S. N. Li, M. Y. Zhang and H. B. Shi, A hydrogen sulphide-responsive and depleting nanoplatform for cancer photodynamic therapy, *Nat. Commun.*, 2022, **13**, 1685.
34 Y. Zhu, Y. Matsumura, M. Velayutham, L. M. Foley, T. K. Hitchens and W. R. Wagner, Reactive oxygen species scavenging with a biodegradable, thermally responsive hydrogel compatible with soft tissue injection, *Biomater. Sci.*, 2018, **177**, 98–112.
35 D. L. Sai, J. Lee, D. L. Nguyen and Y.-P. Kim, Tailoring photosensitive ROS for advanced photodynamic therapy, *Exp. Mol. Med.*, 2021, **53**, 495–504.
36 Q. Xin, H. Shah, A. Nawaz, W. J. Xie, M. Z. Akram, A. Batool, L. Q. Tian, S. U. Jan, R. Boddula, B. D. Guo,

Q. Liu and J. R. Gong, Antibacterial carbon-based nanomaterials, *Adv. Mater.*, 2018, **31**, 1804838.

37 H. W. Ji, H. J. Sun and X. G. Qu, Antibacterial applications of graphene-based nanomaterials: recent achievements and challenges, *Adv. Drug Delivery Rev.*, 2016, **105**, 176–189.

38 S. Joshi, R. Siddiqui, P. Sharma, R. Kumar, G. Verma and A. Saini, Green synthesis of peptide functionalized reduced graphene oxide (rGO) nano bioconjugate with enhanced antibacterial activity, *Sci. Rep.*, 2020, **10**, 9441.

39 J. H. Li, G. Wang, H. Q. Zhu, M. Zhang, X. H. Zheng, Z. D. Di, X. Y. Liu and X. Wang, Antibacterial activity of large-area monolayer graphene film manipulated by charge transfer, *Sci. Rep.*, 2014, **4**, 4359.

40 X. M. Dai, Y. Zhao, Y. J. Yu, X. L. Chen, X. S. Wei, X. G. Zhang and C. X. Li, All-in-one NIR-activated nanoplatforms for enhanced bacterial biofilm eradication, *Nanoscale*, 2018, **10**, 18520.

41 S. Syama and P. V. Mohanan, Comprehensive application of graphene: emphasis on biomedical concerns, *Nano-Micro Lett.*, 2019, **11**, 6.

42 X. H. Chu, P. Zhang, Y. L. Wang, B. H. Sun, Y. H. Liu, Q. C. Zhang, W. L. Feng, Z. H. Li, K. H. Li, N. L. Zhou and J. Shen, Near-infrared carbon dot-based platform for bioimaging and photothermal/photodynamic/quaternary ammonium triple synergistic sterilization triggered by single NIR light source, *Carbon*, 2021, **176**, 126–138.

43 C. B. Leng, X. Zhang, F. X. Xu, Y. Yuan, H. Pei, Z. H. Sun, L. Li and Z. H. Bao, Engineering gold nanorod-copper sulfide heterostructures with enhanced photothermal conversion efficiency and photostability, *Small*, 2018, **14**, 1703077.

44 Y. Zhang, H. J. Yan, J. W. Tang, P. Y. Li, R. X. Su, H. Y. Zhong and W. Su, Dual-mode antibacterial core-shell gold nanorod@mesoporous-silica/curcumin nanocomplexes for efficient photothermal and photodynamic therapy, *J. Photochem. Photobiol., A*, 2022, **425**, 113722.

45 M. P. Brynildsen, J. A. Winkler, C. S. Spina, I. C. MacDonald and J. J. Collins, Potentiating antibacterial activity by predictably enhancing endogenous microbial ROS production, *Nat. Biotechnol.*, 2013, **31**, 160–165.

46 W.-N. Wang, P. Pei, Z.-Y. Chu, B.-J. Chen, H.-S. Qian, Z.-B. Zha, W. Zhou, T. Liu, M. Shao and H. Wang, Bi_2S_3 coated Au nanorods for enhanced photodynamic and photothermal antibacterial activities under NIR light, *Chem. Eng. J.*, 2020, **397**, 125488.

47 O. Akturk, Colloidal stability and biological activity evaluation of microbial exopolysaccharide levan-capped gold nanoparticles, *Colloids Surf., B*, 2020, **192**, 111061.

48 P. Sivakumar, M. Lee, Y.-S. Kim and M. S. Shim, Photo-triggered antibacterial and anticancer activities of zinc oxide nanoparticles, *J. Mater. Chem. B*, 2018, **6**, 4852–4871.

49 H. Li, M. H. Gong, J. Y. Xiao, L. Hai, Y. Z. Luo, L. D. He, Z. F. Wang, L. Deng and D. G. He, Photothermally activated multifunctional MoS_2 bactericidal nanoplatform for combined chemo/photothermal/photodynamic triple-mode therapy of bacterial and biofilm infections, *Chem. Eng. J.*, 2022, **429**, 132600.

50 Z. B. Xu, Z. Y. Qiu, Q. Liu, Y. X. Huang, D. D. Li, X. G. Shen, K. L. Fan, J. Q. Xi, Y. H. Gu, Y. Tang, J. Jiang, J. L. Xu, J. Z. He, X. F. Gao, Y. Liu, H. Koo, X. Y. Yan and L. Z. Gao, Converting organosulfur compounds to inorganic polysulfides against resistant bacterial infections, *Nat. Commun.*, 2018, **9**, 3713.

51 X. M. Dai, Y. Zhao, Y. J. Yu, X. L. Chen, X. S. Wei, X. G. Zhang and C. X. Li, Single continuous near-infrared laser-triggered photodynamic and photothermal ablation of antibiotic-resistant bacteria using effective targeted copper sulfide nanoclusters, *ACS Appl. Mater. Interfaces*, 2017, **9**, 30470–30479.

52 X. Hou, T. L. Shi, C. H. Wei, H. Zeng, X. G. Hu and B. Yan, A 2D–2D heterojunction Bi_2WO_6/WS_{2-x} as a broad-spectrum bactericide: Sulfur vacancies mediate the interface interactions between biology and nanomaterials, *Biomaterials*, 2020, **243**, 119937.

53 S. D. Mo, Y. H. Song, M. H. Lin, J. L. Wang, Z. Zhang, J. Y. Sun, D. G. Guo and L. Liu, Near-infrared responsive sulfur vacancy-rich CuS nanosheets for efficient antibacterial activity via synergistic photothermal and photodynamic pathways, *J. Colloid Interface Sci.*, 2022, **608**, 2896–2906.

54 Z. X. Ling, Z. K. Chen, J. Deng, Y. F. Wang, B. Yuan, X. Yang, H. Lin, J. Cao, X. D. Zhu and X. D. Zhang, A novel self-healing polydopamine-functionalized chitosan-arginine hydrogel with enhanced angiogenic and antibacterial activities for accelerating skin wound healing, *Chem. Eng. J.*, 2020, **420**, 130302.

55 C. Y. Mao, Y. M. Xiang, X. M. Liu, Y. F. Zheng, K. W. K. Yeung, Z. D. Cui, X. J. Yang, Z. Y. Li, Y. Q. Liang, S. L. Zhu and S. L. Wu, Local photothermal/photodynamic synergistic therapy by disrupting bacterial membrane to accelerate reactive oxygen species permeation and protein leakage, *ACS Appl. Mater. Interfaces*, 2019, **11**, 17902–17914.

56 R. Misra and T. K. Chandrashekar, Structural diversity in expanded porphyrins, *Acc. Chem. Res.*, 2008, **41**, 265–279.

57 H. Hu, H. Wang, Y. C. Yang, J.-F. Xu and X. Zhang, A bacteria-responsive porphyrin for adaptable photodynamic/photothermal therapy, *Angew. Chem., Int. Ed.*, 2022, **61**, e202200799.

58 B. H. Sun, Z. Q. Ye, M. Zhang, Q. X. Song, X. H. Chu, S. R. Gao, Q. C. Zhang, C. Jiang, N. L. Zhou, C. Yao and J. Shen, Light-activated biodegradable covalent organic framework-integrated heterojunction for photodynamic, photothermal, and gaseous therapy of chronic wound infection, *ACS Appl. Mater. Interfaces*, 2021, **13**, 42396–42410.

59 P. Ran, H. Zheng, W. X. Cao, X. W. Jia, G. Y. Zhang, Y. Liu and X. H. Li, On-demand changeable theranostic hydrogels and visual imaging-guided antibacterial photodynamic therapy to promote wound healing, *ACS Appl. Mater. Interfaces*, 2022, **14**, 49375–49388.

60 G. C. Qing, X. X. Zhao, N. Q. Gong, J. Chen, X. L. Li, Y. L. Gan, Y. C. Wang, Z. Zhang, Y. X. Zhang, W. S. Guo, Y. Luo and X.-J. Liang, Thermo-responsive triple-function nanotransporter for efficient chemo-photothermal therapy

of multidrug-resistant bacterial infection, *Nat. Commun.*, 2019, **10**, 4336.

61 K. M. Mickiewicz, Y. Kawai, L. Drage, M. C. Gomes, F. Davison, R. Pickard, J. Hall, S. Mostowy, P. D. Aldridge and J. Errington, Possible role of L-form switching in recurrent urinary tract infection, *Nat. Commun.*, 2019, **10**, 4379.

62 Y. Kawai, K. Mickiewicz and J. Errington, Lysozyme counteracts beta-lactam antibiotics by promoting the emergence of L-form bacteria, *Cell*, 2018, **172**, 1038–1049.

63 J. Feng, Z. Xu, P. Dong, W. Q. Yu, F. Liu, Q. Y. Jiang, F. A. Wang and X. Q. Liu, Stimuli-responsive multifunctional metal-organic framework nanoparticles for enhanced chemo-photothermal therapy, *J. Mater. Chem. B*, 2019, **7**, 994–1004.

64 C. X. Sui, R. Tan, Y. W. Chen, G. T. Yin, Z. Y. Wang, W. G. Xu and X. F. Li, MOFs-derived Fe–N co-doped carbon nanoparticles as O_2-evolving reactor and ROS generator for CDT/PDT/PTT synergistic treatment of tumors, *Bioconjugate Chem.*, 2021, **32**, 318–327.

65 X. L. Yin, S. Y. Ran, H. Y. Cheng, M. Zhang, W. Sun, Y. Wan, C. S. Shao and Z. H. Zhu, Polydopamine-modified ZIF-8 nanoparticles as a drug carrier for combined chemo-photothermal osteosarcoma therapy, *Colloids Surf., B*, 2022, **216**, 112507.

66 H. Z. Guo, L. S. Liu, Q. Q. Hu and H. J. Dou, Monodisperse ZIF-8@dextran nanoparticles co-loaded with hydrophilic and hydrophobic functional cargos for combined near-infrared fluorescence imaging and photothermal therapy, *Acta Biomater.*, 2022, **137**, 290–304.

67 X. R. Deng, S. Liang, X. C. Cai, S. S. Huang, Z. Y. Cheng, Y. S. Shi, M. L. Pang, P. A. Ma and J. Lin, Yolk–shell structured Au nanostar@metal–organic framework for synergistic chemo-photothermal therapy in the second near-infrared window, *Nano Lett.*, 2019, **19**, 6772–6780.

68 Z. F. Wang, Y. L. Peng, Y. Zhou, S. N. Zhang, J. X. Tan, H. Li, D. G. He and L. Deng, Pd-Cu nanoalloy for dual stimuli-responsive chemo-photothermal therapy against pathogenic biofilm bacteria, *Acta Biomater.*, 2022, **137**, 276–289.

69 Y. Sun, J. J. Liu, H. Y. Wang, S. S. Li, X. T. Pan, B. L. Xu, H. L. Yang, Q. Y. Wu, W. X. Li, X. Su, Z. J. Huang, X. D. Guo and H. Y. Liu, NIR laser-triggered microneedle-based liquid band-aid for wound care, *Adv. Funct. Mater.*, 2021, **31**, 2100218.

70 J. H. Xu, R. Danehy, H. W. Cai, Z. Ao, M. Pu, A. Nusawardhana, D. Rowe-Magnus and F. Guo, Microneedle patch-mediated treatment of bacterial biofilms, *ACS Appl. Mater. Interfaces*, 2019, **11**, 14640–14646.

71 X. Q. Yu, J. Zhao and D. D. Fan, A dissolving microneedle patch for antibiotic/enzymolysis/photothermal triple therapy against bacteria and their biofilms, *Chem. Eng. J.*, 2022, **437**, 135475.

72 Y. W. Zheng, Y. L. Yan, L. M. Lin, Q. He, H. H. Hu, R. Luo, D. Y. Xian, J. Y. Wu, Y. Shi, F. P. Zeng, C. B. Wu, G. L. Quan and C. Lu, Titanium carbide MXene-based hybrid hydrogel for chemo-photothermal combinational treatment of localized bacterial infection, *Acta Biomater.*, 2022, **142**, 113–123.

73 F. F. Cao, E. G. Ju, Y. Zhang, Z. Z. Wang, C. Q. Liu, W. Li, Y. Y. Huang, K. Dong, J. S. Ren and X. G. Qu, An efficient and benign antimicrobial depot based on silver-infused MoS_2, *ACS Nano*, 2017, **11**, 4651–4659.

74 S. Chernousova and M. Epple, Silver as antibacterial agent: ion, nanoparticle, and metal, *Angew. Chem., Int. Ed.*, 2013, **52**, 1636–1653.

75 K. Y. Zheng, M. I. Setyawati, T.-P. Lim, D. T. Leong and J. P. Xie, Antimicrobial cluster bombs: silver nanoclusters packed with daptomycin, *ACS Nano*, 2016, **10**, 7934–7942.

76 P. V. AshaRani, G. L. K. Mun, M. P. Hande and S. Valiyaveettil, Cytotoxicity and genotoxicity of silver nanoparticles in human cells, *ACS Nano*, 2009, **3**, 279–290.

77 S. Rtimi, D. D. Dionysiou, S. C. Pillai and J. Kiwi, Advances in catalytic/photocatalytic bacterial inactivation by nano Ag and Cu coated surfaces and medical devices, *Appl. Catal., B*, 2019, **240**, 291–318.

78 M. L. Liu, D. F. He, T. Yang, W. Liu, L. Mao, Y. Zhu, J. Wu, G. X. Luo and J. Deng, An efficient antimicrobial depot for infectious site-targeted chemo-photothermal therapy, *J. Nanobiotechnol.*, 2018, **16**, 23.

79 F. Rong, Y. Z. Tang, T. J. Wang, T. Feng, J. Song, P. Li and W. Huang, Nitric oxide-releasing polymeric materials for antimicrobial applications: a review, *Antioxidants*, 2019, **8**, 556.

80 B. H. Zhao, H. Wang, W. J. Dong, S. W. Cheng, H. S. Li, J. L. Tan, J. Y. Zhou, W. F. He, L. L. Li, J. X. Zhang, G. X. Luo and W. Qian, A multifunctional platform with single-NIR-laser-triggered photothermal and NO release for synergistic therapy against multidrug-resistant Gram-negative bacteria and their biofilms, *J. Nanobiotechnol.*, 2020, **18**, 59.

81 A. Galstyan, R. Schiller and U. Dobrindt, Boronic acid functionalized photosensitizers: a strategy to target the surface of bacteria and implement active agents in polymer coatings, *Angew. Chem., Int. Ed.*, 2017, **56**, 10362–10366.

82 K. K. Behara, Y. Rajesh, Y. Venkatesh, B. R. Pinninti, M. Mandal and N. D. P. Singh, Cascade photocaging of diazeniumdiolate: a novel strategy for one and two photon triggered uncaging with real time reporting, *Chem. Commun.*, 2017, **53**, 9470–9473.

83 S. M. Yu, G. W. Li, R. Liu, D. Ma and W. Xue, Dendritic Fe_3O_4@poly(dopamine)@PAMAM nanocomposite as controllable NO-releasing material: A synergistic photothermal and NO antibacterial study, *Adv. Funct. Mater.*, 2018, **28**, 1707440.

84 Q. Gao, X. Zhang, W. Y. Yin, D. Q. Ma, C. J. Xie, L. R. Zheng, X. H. Dong, L. Q. Mei, J. Yu, C. Z. Wang, Z. J. Gu and Y. L. Zhao, Functionalized MoS_2 nanovehicle with near-infrared laser mediated nitric oxide release and photothermal activities for advanced bacteria-infected wound therapy, *Small*, 2018, **14**, 1802290.

85 Z. Y. Liang, W. K. Liu, Z. Q. Wang, P. L. Zheng, W. Liu, J. F. Zhao, Y. L. Zhong, Y. Zhang, J. Lin, W. Xue and

S. M. Yu, Near-infrared laser-controlled nitric oxide-releasing gold nanostar/hollow polydopamine janus nanoparticles for synergistic elimination of methicillin-resistant Staphylococcus aureus and wound healing, *Acta Biomater.*, 2022, **143**, 428–444.

86 C. X. Sun, B. H. Li, M. Y. Zhao, S. F. Wang, Z. H. Lei, L. F. Lu, H. X. Zhang, L. S. Feng, C. R. Dou and D. R. Yin, J-aggregates of cyanine dye for NIR-II in vivo dynamic vascular imaging beyond 1500 nm, *J. Am. Chem. Soc.*, 2019, **141**, 19221–19225.

87 S. Xu, H.-W. Liu, S.-Y. Huan, L. Yuan and X.-B. Zhang, Recent progress in utilizing near-infrared J-aggregates for imaging and cancer therapy, *Mater. Chem. Front.*, 2021, **5**, 1076–1089.

88 Y. F. Chen, X. H. Zhang, D. B. Cheng, Y. J. Zhang, Y. Liu, L. Ji, R. C. Guo, H. Chen, X. K. Ren, Z. J. Chen, Z. Y. Qiao and H. Wang, Near-infrared laser-triggered in situ dimorphic transformation of BF_2-azadipyrromethene nanoaggregates for enhanced solid tumor penetration, *ACS Nano*, 2020, **14**, 3640–3650.

89 O. Flores, J. Pliquett, L. A. Galan, R. Lescure, F. Denat, O. Maury, A. Pallier, P.-S. Bellaye, B. Collin, S. Même, C. S. Bonnet, E. Bodio and C. Goze, Aza-BODIPY platform: toward an efficient water-soluble bimodal imaging probe for MRI and near-infrared fluorescence, *Inorg. Chem.*, 2020, **59**, 1306–1314.

90 X. Y. Bao, S. Q. Zheng, L. Zhang, A. Z. Shen, G. Y. Zhang, S. Y. Liu and J. M. Hu, Nitric oxide-releasing aza-BODIPY: A new near-infrared J-aggregate with multiple antibacterial modalities, *Angew. Chem., Int. Ed.*, 2022, **61**, e202207250.

91 D. M. Xi, M. Xiao, J. F. Gao, L. Y. Zhao, N. Xu, S. R. Long, J. L. Fan, K. Shao, W. Sun, X. H. Yan and X. J. Peng, NIR light-driving barrier-free group rotation in nanoparticles with an 88.3% photothermal conversion efficiency for photothermal therapy, *Adv. Mater.*, 2020, **32**, 1907855.

92 J. J. Huo, Q. Y. Jia, H. Huang, J. Zhang, P. Li, X. C. Dong and W. Huang, Emerging photothermal-derived multimodal synergistic therapy in combating bacterial infections, *Chem. Soc. Rev.*, 2021, **50**, 8762–8789.

93 R. H. Wang, Q. W. Liu, A. Gao, N. Tang, Q. Zhang, A. Zhang and D. X. Cui, Recent developments of sonodynamic therapy in antibacterial application, *Nanoscale*, 2022, **14**, 12999.

94 X. L. Bi, Q. Bai, M. M. Liang, D. Q. Yang, S. H. Li, L. Wang, J. Liu, W. W. Yu, N. Sui and Z. L. Zhu, Silver peroxide nanoparticles for combined antibacterial sonodynamic and photothermal therapy, *Small*, 2022, **18**, 2104160.

95 W. T. He, S. F. Hu, X. L. Du, Q. Wen, X.-P. Zhong, X. Y. Zhou, C. Y. Zhou, W. J. Xiong, Y. C. Gao, S. M. Zhang, R. N. Wang, J. H. Yang and L. Ma, Vitamin B5 reduces bacterial growth via regulating innate immunity and adaptive immunity in mice infected with mycobacterium tuberculosis, *Front. Immunol.*, 2018, **9**, 365.

96 Q. Zhao, J. Y. Wang, C. C. Yin, P. Zhang, J. L. Zhang, M. S. Shi, K. L. Shen, Y. Xiao, Y. B. Zhao, X. L. Yang and Y. F. Zhang, Near-infrared light-sensitive nano neuroimmune blocker capsule relieves pain and enhances the innate immune response for necrotizing infection, *Nano Lett.*, 2019, **19**, 5904–5914.

97 Y. Li, X. M. Xu, X. M. Liu, B. Li, Y. Han, Y. F. Zheng, D.-F. Chen, K. W. K. Yeung, Z. D. Cui, Z. Y. Li, Y. Q. Liang, S. L. Zhu, X. B. Wang and S. L. Wu, Photoelectrons mediating angiogenesis and immunotherapy through heterojunction film for noninvasive disinfection, *Adv. Sci.*, 2020, **7**, 2000023.

98 Y. J. Tian, Y. Li, J. L. Liu, Y. Lin, J. Jiao, B. Chen, W. M. Wang, S. L. Wu and C. Y. Li, Photothermal therapy with regulated Nrf2/NF-κB signaling pathway for treating bacteria-induced periodontitis, *Bioact. Mater.*, 2022, **9**, 428–445.

99 M. Zhu, X. Liu, L. Tan, Z. D. Cui, Y. Liang, Z. Li, K. W. K. Yeunga and S. L. Wu, Photo-responsive chitosan/Ag/MoS_2 for rapid bacteria-killing, *J. Hazard. Mater.*, 2020, **383**, 121122.

100 X. Yu, D. He, X. Zhang, H. Zhang, J. Song, D. Shi, Y. Fan, G. Luo and J. Deng, Surface-adaptive and initiator-loaded graphene as a light-induced generator with free radicals for drug-resistant bacteria eradication, *ACS Appl. Mater. Interfaces*, 2019, **11**, 1766–1781.

101 P. Teratanatorn, R. Hoskins, T. Swift, C. W. I. Douglas, J. Shepherd and S. Rimmer, Binding of bacteria to poly-(N-isopropylacrylamide) modified with vancomycin: Comparison of behavior of linear and highly branched polymers, *Biomacromolecules*, 2017, **18**, 2887–2899.

102 Y. Q. Wang, Y. Y. Jin, W. Chen, J. J. Wang, H. Chen, L. Sun, X. Li, J. Ji, Q. Yu, L. Y. Shen and B. L. Wang, Construction of nanomaterials with targeting phototherapy properties to inhibit resistant bacteria and biofilm infections, *Chem. Eng. J.*, 2019, **358**, 74–90.

103 Z. Xu, B. Deng, X. W. Wang, J. Yu, Z. B. Xu, P. G. Liu, C. H. Liu, Y. Cai, F. Wang, R. L. Zong, Z. L. Chen and H. Xing, Nanofiber-mediated sequential photothermal antibacteria and macrophage polarization for healing MRSA-infected diabetic wounds, *J. Nanobiotechnol.*, 2021, **19**, 404.

